



RESEARCH ARTICLE

Plant–soil interactions alter nitrogen and phosphorus dynamics in an advancing subarctic treeline

Jasmin Fetzer^{1,2}  | Pavel Moiseev³  | Emmanuel Frossard²  | Klaus Kaiser⁴  |
Mathias Mayer^{1,5,6}  | Konstantin Gavazov¹  | Frank Hagedorn¹ 

¹Forest Soils and Biogeochemistry, Swiss Federal Institute for Forest, Snow and Landscape Research WSL, Birmensdorf, Switzerland

²Department of Environmental Systems Science, ETH Zurich, Zürich, Switzerland

³Institute of Plant and Animal Ecology, Ekaterinenburg, Russia

⁴Soil Science and Soil Protection, Martin Luther University Halle-Wittenberg, Halle (Saale), Germany

⁵Department of Forest and Soil Sciences, Institute of Forest Ecology, University of Natural Resources and Life Sciences (BOKU), Vienna, Austria

⁶Forest Ecology, Institute of Terrestrial Ecosystems (ITES), ETH Zurich, Zurich, Switzerland

Correspondence

Frank Hagedorn, Forest Soils and Biogeochemistry, Swiss Federal Institute for Forest, Snow and Landscape Research WSL, Birmensdorf, Switzerland.
Email: frank.hagedorn@wsl.ch

Funding information

Schweizerischer Nationalfonds zur Förderung der Wissenschaftlichen Forschung, Grant/Award Number: 171171 and PZ00P2_174047; Deutsche Forschungsgemeinschaft, Grant/Award Number: KA1673/9-2; Austrian Science Fund, Grant/Award Number: J-4369

Abstract

Treelines advance due to climate warming. The impacts of this vegetation shift on plant–soil nutrient cycling are still uncertain, yet highly relevant as nutrient availability stimulates tree growth. Here, we investigated nitrogen (N) and phosphorus (P) in plant and soil pools along two tundra–forest transects on Kola Peninsula, Russia, with a documented elevation shift of birch-dominated treeline by 70 m during the last 50 years. Results show that although total N and P stocks in the soil–plant system did not change with elevation, their distribution was significantly altered. With the transition from high-elevation tundra to low-elevation forest, P stocks in stones decreased, possibly reflecting enhanced weathering. In contrast, N and P stocks in plant biomass approximately tripled and available P and N in the soil increased fivefold toward the forest. This was paralleled by decreasing carbon (C)-to-nutrient ratios in foliage and litter, smaller C:N:P ratios in microbial biomass, and lower enzymatic activities related to N and P acquisition in forest soils. An incubation experiment further demonstrated manifold higher N and P net mineralization rates in litter and soil in forest compared to tundra, likely due to smaller C:N:P ratios in decomposing organic matter. Overall, our results show that forest expansion increases the mobilization of available nutrients through enhanced weathering and positive plant–soil feedback, with nutrient-rich forest litter releasing greater amounts of N and P upon decomposition. While the low N and P availability in tundra may retard treeline advances, its improvement toward the forest likely promotes tree growth and forest development.

KEYWORDS

biogeochemistry, climate change, elevation gradient, extracellular enzymatic activity, forest, microbial biomass, nutrient cycling, stoichiometry, tundra

1 | INTRODUCTION

Treelines are one of the most striking natural vegetation boundaries, where low stature plants, dwarf shrubs, or grasses transition into areas of upright growing trees. In unmanaged regions, the

position of the treeline is mainly determined by low temperatures during the vegetation period constraining tree growth (e.g., Körner & Paulsen, 2004). The strong climatic warming at high latitudes and elevations (Pepin et al., 2015) has relieved some of the temperature constraints, inducing an upward shift of treeline in most mountain

This is an open access article under the terms of the [Creative Commons Attribution](https://creativecommons.org/licenses/by/4.0/) License, which permits use, distribution and reproduction in any medium, provided the original work is properly cited.

© 2024 The Authors. *Global Change Biology* published by John Wiley & Sons Ltd.

ranges (Harsch et al., 2009). However, treeline advances lag behind temperature increases on mountains due to other factors controlling tree growth such as plant competition, forest demography, and nutrient availability (Hagedorn et al., 2019; Liang et al., 2016; Sullivan et al., 2015). Fertilization experiments at treelines and in tundra ecosystem show pronounced responses of plant growth to low doses of nutrient additions (Möhl et al., 2018), indicating that nutrient availability can play an important role for treeline dynamics in a warming climate. Due to small mineralization rates at low temperatures and the primary storage of nitrogen (N) in soil organic matter (SOM), cold ecosystems are assumed to be predominantly nitrogen limited (Augusto et al., 2017; Hagedorn et al., 2019). Increasing temperatures may, however, lead to higher N availability due to faster N mineralization as observed in a 6-year long soil warming experiment at treeline (Dawes, Schleppi, Hättenschwiler, et al., 2017). Less is known about phosphorus (P) dynamics at treeline, but the availability of P might also be important in biologically inactive and poorly weathered soils (Celi et al., 2013; Welc et al., 2014).

In addition to the nutrient supply from parent material, nutrient cycling and soil nutrient availabilities in a given or changing vegetation are shaped by plant–soil interactions operating at various timescales (Bowman et al., 2004; Hagedorn et al., 2019; Van Breemen & Finzi, 1998). These interactions may encompass (1) litter feedbacks due to a distinct plant-specific litter chemistry and stoichiometry (Elser et al., 2010), which in turn control net nutrient mineralization and microbial immobilization (Mooshammer et al., 2014); (2) the influence of canopy structures on microclimatic conditions driving biogeochemical processes (Kammer et al., 2009; Seastedt & Adams, 2001); and (3) nutrient uptake by plants and storage of “available” nutrients in biomass (Lovett et al., 2018; Vitousek & Reiners, 1975). Longer term plant–soil feedbacks include (4) the formation of SOM characteristic for a vegetation type (i.e., accumulation of an organic layer); (5) the mining by roots and associated mycorrhizal fungi for nutrients (Clemmensen et al., 2021); and (6) vegetation effects on weathering, either directly by rhizosphere activity or indirectly by soil abiotic conditions (Van Breemen & Finzi, 1998).

Despite the striking climate-related shift in plant life forms and species across treeline ecotones, plant–soil feedbacks therein have rarely been studied comprehensively. In seven disparate montane regions around the globe, concentrations of available N and P have been found to increase from tundra toward forests, which was primarily attributed to elevational changes in soil C:N ratios (Mayor et al., 2017). In support, litter decomposition studies reveal faster decomposition and higher nutrient mass loss from forest than from tundra litter (Hagemann & Moroni, 2015; Wang et al., 2021), suggesting that litter feedbacks contribute to the improving nutrient availability from forest to tundra. However, in contrast to this notion, N availability was found to decrease from a heath tundra toward a birch forest at a sub-arctic treeline in Northern Sweden (Clemmensen et al., 2021; Parker et al., 2015). While these studies have measured specific aspects of nutrient cycling at treeline, a holistic assessment on the impacts of treeline shifts on nutrient dynamics is still lacking.

For instance, results from process-based studies (e.g., litter decomposition) have not been linked to assessments of soil nutrient availability based on soil extracts and nutrient contents in plant foliage. Moreover, gradient studies have determined nutrient concentrations in topsoil extracts as well as in plant foliage as indicators for nutrient availability instead of quantifying pool sizes of nutrients in entire soil profiles and plant biomass. To our knowledge, patterns in soil weathering have not been studied across treelines although ectomycorrhizal fungi associated with trees have a high capability to solubilize elements from parent materials (Van Breemen & Finzi, 1998), which would be particularly relevant for P. While most studies are based on the “space-for-time substitution approach” to climate change, making use of either elevational gradients (e.g., Mayor et al., 2017) or paired plots (Clemmensen et al., 2021), in stark contrast to this study, they lack a documented forest expansion at the study sites, which limits mechanistic assessments of the feedback between treeline advances and soil nutrient cycling.

Our study aimed (1) to quantify how ecosystem pools and cycling of N and P change across a subarctic forest–tundra ecotone, (2) to assess how they are affected by an upward shift in forest vegetation, and (3) how changes in nutrient cycling feedback on treeline dynamics. We sampled plants and soils along two transects spanning 200 m in elevation in the Khibiny mountains on Kola Peninsula, Russia (Moiseev et al., 2019), reaching from birch forests to tree-free mountain tundra. On the same transects, dendrochronological analysis documented that the forest is expanding upward (Moiseev et al., 2019). Over the last 50–60 years, the upper boundary of open forest shifted upward by 50–80 m and forests became significantly denser due to climate warming, representing an increase in summer temperature by 0.9–1.3°C and a lengthening of the growing season by 5–10 days during the last century (Kononov et al., 2009; Moiseev et al., 2019). In other Eurasian mountains (Polar Urals), reconstructions of treeline dynamics based on fossil wood indicated that, during the last millennia, treelines have been shifting by about 80 m in elevation with the current treeline reaching similar elevations as during the medieval warm period between the 11th and 13th centuries (Shiyatov & Mazepa, 2011). We are therefore confident that our elevational gradient comprised sites that have been tundra and forest for at least centuries, but also sites that experienced a shift from tundra to trees within the last decades. This unique experimental setup allowed us to study not only long-term plant–soil interactions but also short-term effects of vegetation shifts on soil nutrient dynamics in this subarctic forest–tundra ecotone.

We hypothesized treelines to represent a distinct boundary for nutrient cycling changing from tundra at high elevation toward forest at lower elevation by:

Hypothesis 1. A positive litter feedback, where trees and understory plants in forest produce more and higher quality foliage and litter with narrower C:N:P ratios than in tundra. In conjunction with a more favorable microclimate in the forest, this causes faster

litter decomposition, as well as greater net N and P mineralization in forest soils.

Hypothesis 2. Positive plant–soil feedbacks with trees enhancing weathering and soil development, which shifts the P-pool distribution from parent material into plant available pools with forest development.

Hypothesis 3. A negative plant–soil feedback by an increasing uptake of available soil N and P and their accumulation and immobilization in tree biomass from tundra toward the low elevation forest, which might counterbalance to some extent the improving N and P nutrition as hypothesized above.

To test our hypotheses, we analyzed a set of biogeochemical variables across the treeline ecotone allowing to comprehensively assess nutrient cycling. These measurements included (i) soil temperature, soil depths, contents, and mineralogy of stones to characterize weathering; (ii) N and P pools in the soil encompassing stones, fine earth, as well plant-available N and P forms; (iii) biomass and elemental composition of plant components to estimate plant nutrient pool sizes and stoichiometry; and finally (iv) net N and P mineralization from litter and topsoils, microbial biomass, and its C:N:P ratio, as well as extracellular enzyme activity to elucidate nutrient mobilization and immobilization by microbial communities.

2 | MATERIALS AND METHODS

2.1 | Study site

The study area is located in a treeline ecotone in the Khibiny Mountains, Kola Peninsula, Northern Russia (67°35'N, 34°04'E, Figure 1). The Khibiny massif is a mafic pluton with high contents of apatite (Kogarko, 2018). Climate depends on the continuously ice-free Northern Atlantic Ocean and Barents Sea with snow-rich winter and cool and cloudy summers. Mean annual temperature is −3.7°C, while average annual precipitation amounts to 928 mm and shows an even distribution with one-third falling in June until September. The region is snow covered from October to May (Mathisen et al., 2014; Moiseev et al., 2019).

Sampling took place on an elevational gradient covering ecosystem succession from mountain tundra to mature boreal birch forest. The tundra above treeline is a dwarf shrub lichen heath (Makarov et al., 2019; Ushakova et al., 2003) mainly consisting of dwarf shrubs, grasses, mosses, and lichens (for the species list, refer to Table S1). The dominant species at the treeline is *Betula pubescens* ssp. *czerepanovii*. Toward the low-elevation forest, there is an increasing contribution of Siberian spruce (*Picea obovata* Ledeb.) growing in patches. Their coverage remains, however, below 15%. At the current treeline, trees are ~50 years old, and tree age doubles up to ~100 years at 60 m below the treeline (Moiseev et al., 2019). At the treeline and in forest areas, the understory is dominated by *Vaccinium* spp. intermixed with ferns and grasses.

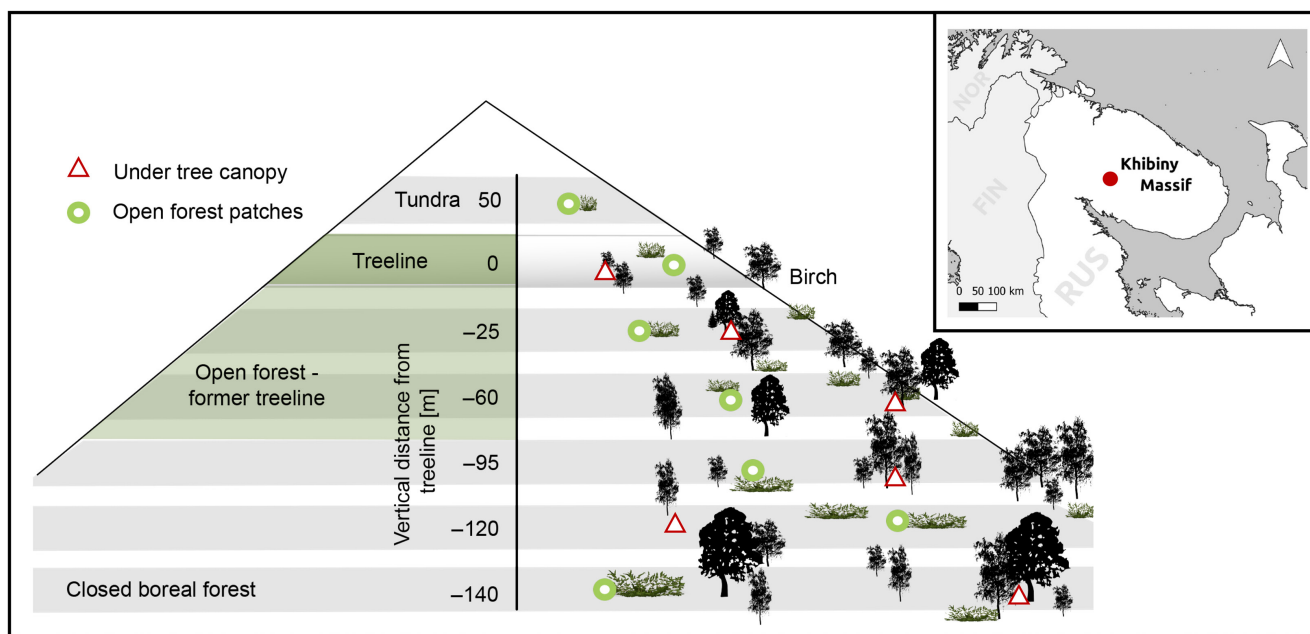


FIGURE 1 Design of the elevational transects in the Khibiny Massif, Kola Peninsula, Russia. Two transects from tundra to boreal forest dominated by birch were set up (~1 km apart from each other) with seven elevational levels each. Sampling was done at each elevational level below “tree canopies” (triangle) and in “open areas” either in the tundra or in forest patches (circle). “Former treeline”: area in which the treeline advanced during the last 50–60 years, as estimated by Mathisen et al. (2014) and Moiseev et al. (2019). The map was extracted from the GADM database (www.gadm.org), map lines delineate study areas and do not necessarily depict accepted national boundaries.

The soils in the study area developed from the same parent material and are of similar age of ~8.5–7.5 thousand years (Pekala, 1998). Along the elevation gradient, they ranged from cryoturbated Gelic Leptosols in tundra above treeline to Haplic Podzols in the boreal forest at lower elevation (WRB, 2014, Figure S1).

2.2 | Sampling

2.2.1 | Sampling design

At the end of July 2017, we established two elevation transects ranging from the tundra to the boreal forest. Transects were south-east facing and gently sloping (4–5°) and reached from 470 to 280 m a.s.l. The horizontal distance between transects was ~1000 m. Along each transect, seven elevational levels were defined for further sampling; spanning from the tundra being 50 vertical meter above the treeline, to the current treeline at ~400 m a.s.l. (canopy cover ~5%), the open forest with a canopy cover of 20%–50%, and the closed forest (canopy cover >50%) at the lowest elevational level, which was 140 m vertically below the treeline. The treeline was defined as the elevation, where the highest upright growing trees (>2 m) were found growing in tree islands in the tundra vegetation. Below the treeline, samples were taken at five elevational levels with increasing stand densities (Figure 1). Sampling was carried out at three to five plots at each elevational level. Within each plot, we dug two soil pits, one under the canopy of birch trees, ~2–4 m away from stem (hereafter referred to as “tree canopy” plots) and one in the surrounding open land at a distance of at least 5 m from the tree canopy (hereafter referred to as “open area” plots). The open area plots comprised tundra-type vegetation at the highest three elevational levels and a mixture of dwarf shrubs and herbaceous species at the four lower levels, respectively.

2.2.2 | Climate data

Soil temperature was monitored at four of the seven elevational levels (tundra, treeline, 60 m and 95 m below treeline) with Maxim iButtons (iButton DS1922L-F5; Maxim Integrated, San Jose, USA) from July 2017 to July 2018. Soil temperature sensors were installed in 10 cm soil depth in the A horizon (average rooting zone). Using these data, we calculated length and mean soil temperature of the growing season for each elevation, adopting the 3.2°C soil temperature threshold for defining the beginning and the end of the growing season according to Körner and Paulsen (2004).

2.2.3 | Plant biomass sampling

For biomass estimates, 20 plots of 320 m² each were established along the two transects nearby the soil plots, on which all saplings taller than 20 cm and all trunks of single- or multi-stemmed trees

($n=1545$) were measured for their height, basal diameter of each trunk, and crown diameter (for details, see Moiseev et al., 2022). To estimate aboveground biomass of *B. pubescens*, 53 representative trees were felled and separated into stem, branches, and leaves, as described in Moiseev et al. (2022). After measuring fresh masses, representative subsamples were taken for further analysis; for example, cross-cuts of stems including bark; transported to the laboratory for determining dry masses by drying at 105°C. Allometric functions were then established based on the representative trees which were finally used to estimate the aboveground biomass of forest stands. For belowground biomass, we applied ratios of above- to belowground biomass of *B. pubescens* stands observed in the Northern Urals (Hagedorn et al., 2020). For chemical analysis, leaves from *B. pubescens* were sampled at each elevational level. In addition, leaves from *Vaccinium myrtillus* and *V. uliginosum* ($n=45$) were sampled as they represented the most dominant plant species of the understory vegetation growing at all elevational levels. Leaf samples were dried at 40°C and an aliquot was milled for chemical analysis. In addition, bark and stem wood of *B. pubescens* for chemical analysis were sampled 60 m below treeline.

2.2.4 | Soil sampling

Soil sampling was carried out in July 2017. Volume-based soil samples were taken from the litter horizon (L and F horizon together) and at soil depths of 0–5 cm, 5–10 cm, 10–20 cm, and 20 cm down to the bedrock. Litter layers and mineral topsoils were sampled with a frame of 20 cm × 20 cm, while the depth increment >20 cm was sampled at four locations in each pit using a soil corer with an inner diameter of 2 cm. In addition to the pit depth, a soil auger was used to determine soil depth with 60–70 measurement points per elevational level. Soil and stone volume for each depth layer was determined by measuring the pit's dimensions with a ruler. Stone content of each soil layer was determined by weighing and 12 exemplary samples were taken to the laboratory for mineralogical analysis. The volume of the corer was used to determine bulk density for the four samples per pit in the depth increment >20 cm. In total, 274 soil samples were taken. Soil material was sieved to <4 mm in the field to remove stones and roots. After weighing the total mass of soils, subsamples were taken to the laboratory, where they were sieved to <2 mm; aliquots were freeze-dried for chemical analysis and to determine gravimetric soil water content. Field-moist soil samples were stored at 4°C prior to analysis.

2.3 | Plant and soil analysis

2.3.1 | Plants

Leaves and stem wood of *B. pubescens* and leaves of *Vaccinium* (*V. myrtillus* and *V. uliginosum*) were analyzed for N isotopic composition, and total C, N, and P concentrations. The concentrations of N and C and $\delta^{15}\text{N}$ values were measured using an automated elemental

analyzer–continuous flow isotope ratio mass spectrometer (Euro EA 3000; HEKAtech, Wegberg, Germany, interfaced with Delta-S; Thermo Finnigan, Bremen, Germany). Isotopic compositions are given in delta (δ) notation, representing ‰ relative to atmospheric N_2 for $\delta^{15}N$. Total P concentrations were determined via digestion in $8.3\text{ mol L}^{-1} \text{ HNO}_3$ with $0.6\text{ mol L}^{-1} \text{ HF}$ in a microwave digestion unit (MW ultraCLAV MLS; Milestone, Inc., Shelton, CT, USA) and total P was subsequently measured using ICP-OES (Optima 7300 DV; Perkin Elmer, Waltham, MA, USA).

2.3.2 | Soil

Total C, N, and P were determined for all soil depths. The C and N contents as well as $\delta^{15}N$ were analyzed on freeze-dried soil subsamples as described above. Total P was determined by sequential wavelength-dispersive X-ray fluorescence spectroscopy (S8 Tiger Series 2; Bruker AXS, Karlsruhe, Germany) in fused beads of sample aliquots that were ashed at 1000°C . Fused beads were produced with borate fluxes using a XrFuse 6 electric fusion analyzer (XRF Technology Pty Ltd., Malaga, WA, Australia). The spectrometer's default calibration was used for initial data evaluation. Ten International Soil-analytical Exchange (ISE) reference soils from the Wageningen evaluating programs for analytical laboratories (WEPAL) were also analyzed the same way and the values were plotted against the certified P concentrations. The resulting regression was then used for correction of the sample values derived from the default calibration. Results were also corrected for loss of ignition. Due to little sampling material, samples from Tree and Open plots of each elevational level were pooled.

Soil nitrate and soil ammonium ($\text{NH}_4^+\text{-N}$) concentrations were measured on field-moist soil samples. Fresh soil was extracted with 1 M KCl (soil-extractant ratio: 0–5 cm soil depth 1:10, 5–10 cm depth 1:5) after shaking it overhead for 1.5 h. Suspensions were subsequently passed through filters that were pre-washed twice with ultrapure water. Ammonium was measured photometrically with a FIAS-400 (Perkin-Elmer, Waltham, MA, USA) using ammonium gas diffusion and photometric determination (UV/VIS Spectrometer Lambda 2S; Perkin-Elmer). Nitrate was measured photometrically as well as with ionic chromatography (ICS 3000; Dionex, Sunnyvale, CA, USA). In addition, the pH of the extracts was measured with a 691 pH meter (Metrohm, Herisau, Switzerland) equipped with an LL electrode.

Phosphorus extraction with resin (P_{Resin}) (Hedley & Stewart, 1982; Moir & Tiessen, 2007) was carried out with 0.5 g dry equivalent of field-moist soil and 30 mL of ultra-pure water, followed by colorimetric phosphate determination (UV-1800; Shimadzu, Canby, USA) with the malachite green method of Ohno and Zibilske (1991).

Clay, silt, and sand contents of a subset of samples from the soil depths 10–20 cm were measured by the sedimentation method according to Gee and Bauder (1986).

Soil microbial biomass P was determined by means of the fumigation extraction method (Hedley & Stewart, 1982). Two sets of 1-g

sieved soil subsamples were used. One set was fumigated with liquid hexanol. From both sample sets, P was extracted with an anion exchange resin and phosphate was measured as described above. Soil microbial biomass P was determined as the difference in phosphate of fumigated and non-fumigated samples, respectively. To account for sorption, a third sample set was spiked with P and then extracted following the same procedure. The recovery of spiked P averaging 90% was used to correct microbial P (Hedley & Stewart, 1982).

Soil microbial C and N were determined using two sets of 5-g sieved field-moist soil subsamples. One set was fumigated with $\sim 27\text{ mL}$ of CHCl_3 for 24 h. Fumigated and non-fumigated samples were extracted with $0.5\text{ M K}_2\text{SO}_4$ for 1.5 h (soil-extractant ratio: 0–5 cm depth 1:10, 5–10 cm depth 1:5). After filtering, the extracts were analyzed for dissolved organic carbon (DOC) and total nitrogen (TN) using a Formacs HT/TN analyzer (Skalar, The Netherlands). Microbial biomass C and N were calculated as the difference in DOC and TN of fumigated and non-fumigated samples, respectively.

Potential activities of five hydrolytic extracellular enzymes ($\text{nmol g}^{-1} \text{ dry soil h}^{-1}$) involved in the degradation of SOM were estimated using the microplate fluorometric assay according to German et al. (2011) and Pritsch et al. (2011). As C cycle-related enzymes, we measured the activities of β -glucosidase, *N*-acetylglucosaminidase, and xylosidase. As N and P cycle-related enzymes, we measured leucine-amino-peptidase and phosphomonoesterase, respectively. We added fluorometrically labelled substrates (4-methylumbelliferone and 7-amino-4-methyl coumarin) to water extracts of the soil (natural soil pH of 4.1) and measured absorbance (excitation: 368 nm; emission: 465 nm) after 1, 2.5, and 4 h with a Tecan plate reader (InfiniteM200; Tecan, Männedorf, Switzerland, with software Magellan 7.1 by Tecan). The enzyme activity was calculated by measuring the linear increase in fluorescence with time.

2.3.3 | Phosphorus in stones

The mineral composition of 12 exemplary stone samples was measured with an X-ray diffraction analysis (XRD, X-ray diffractometer D8 Advance; Bruker AXS, Germany) in $\sim 2\text{ g}$ of ground stone material. The stones were collected directly from the pits in two soil depths of 5–10 cm and $>20\text{ cm}$.

2.3.4 | Release of C, N, P

Litter material (10 g of fresh sample cut into $2\text{ cm} \times 1\text{ cm}$ pieces) was incubated over 3 weeks at 15°C in microlysimeters (Millipore Stericup; 250 mL). They were leached weekly with 100 mL nutrient solution ($400\text{ }\mu\text{mol L}^{-1} \text{ CaCl}_2$, $50\text{ }\mu\text{mol L}^{-1} \text{ K}_2\text{SO}_4$, and $50\text{ }\mu\text{mol L}^{-1} \text{ MgSO}_4$; Brödlin, Kaiser, & Hagedorn, 2019; Brödlin, Kaiser, Kessler, & Hagedorn, 2019). Following filtration, ammonium and phosphate concentrations were analyzed in the leachate. Carbon mineralization was determined by placing the microlysimeters into airtight containers (1000 mL) and trapping respired CO_2 in 25 mL of 0.5 M NaOH for

1 week. The amount of CO₂ trapped was determined by immediately measuring the reduction in electrical conductivity calibrated by titration with HCl following BaCl₂ addition. For cumulative C mineralization rates, the concentrations of the three leaching cycles were summed up.

Potential C, N, and P mineralization rates from topsoils were determined from sieved fresh soils (0–5 cm depth) sampled from tundra at the highest elevation and at treeline from both open areas and below tree canopies. Soils were brought to 80% WHC with Milli-Q water and incubated in a dark climate chamber for 21 days at 10°C. Samples the equivalent of 5 g dry weight were placed in 300 mL glass vials and capped with rubber septa. Their headspace was replaced with CO₂-free synthetic air by flushing for 3 min at a 1-L min⁻¹ flow rate. At regular intervals (i.e., 2–3 days), the CO₂ concentration in the vials was determined by recirculating the headspace volume for ~3 min at 250 mL min⁻¹ through a gas spectrometer (Picarro G2131-I, Santa Clara, USA), after which the vials were flushed again. Following corrections for gas temperature and pressure, the cumulative CO₂ concentrations of eight measurement cycles were used to determine the overall soil C mineralization rates. Soil nitrate, ammonium, and phosphate concentrations at the end of the incubation period were determined as above and used thereby to calculate the respective net release rates with reference to the initial concentrations.

2.4 | Data calculations and statistical analysis

Soil carbon and nutrient stocks of each horizon were calculated by multiplying their concentrations with the respective soil mass per m² (volume-based soil sampling) and soil depth. For P, we included stones to estimate total “pedon P stocks” and excluded them to calculate “soil fine earth P stocks”. The mafic parent material was assumed not to contain N. Stocks of plant nutrients were calculated by multiplying their concentrations with the determined biomass per hectare for the transects according to Moiseev et al. (2019, 2022). Pool sizes and N concentration of fine roots were taken from observations at a treeline in the South and Polar Urals (Solly et al., 2017). Understory biomass estimations were also taken from measurements at treeline in the Polar and South Urals and at another site in the Khibiny mountains (Solly et al., 2017; Ushakova et al., 2003). For N and P stocks in understory biomass, it was assumed understory vegetation comprises of 80% branches and 20% leaves (Dawes et al., 2015). Nitrogen and P concentration in branches were taken from Uri et al. (2007). References and assumptions made to estimate N and P stocks in biomass are given in Table S8. To calculate P contents in stones, the measured average F-apatite concentration of 1.1% was used for the whole transect.

Statistical analysis was conducted in R (version 3.6.3, R Core Team, 2020). We used linear mixed effects models to assess the effect of elevation and vegetation on response variables. For that, we used the *lmer()* function from the R package *lme4* (Bates et al., 2015). According to the experimental design, we included elevation as a

continuous variable, vegetation (Tree vs. Open), and soil depth as fixed effects with an interaction between elevation and soil depth. The random effect structure was modeled as following: plots nested in the seven elevation levels, nested in the two transects. As the dataset was unbalanced, type 3 sum of squares was used with the *Anova()* function from the R package *car* (Fox et al., 2019). Due to non-normal distributed residuals, most tested parameters were (log+0.1)-transformed for the statistical analysis. *p*-Values were obtained with the R package *lmerTest* (Kuznetsova et al., 2017) and fixed effects were considered significant at *p* < .05; *p*-values between .05 and .1 were considered as marginally significant. Elevation was estimated as the difference to treeline position, allowing to scale for slight differences between the two transects. To test the effects of tree establishment in the tundra at treeline, we conducted an additional analysis for the uppermost three elevation levels, where vegetation of open areas consisted of tundra plants and trees grew in tree clusters.

3 | RESULTS

3.1 | Climate

Daily soil temperatures ranged from 0.03°C in tundra in April to 14°C in July in the forest at the lowest elevation (Figure 2). Soil temperatures in the rooting zone were consistently higher in the forest than in tundra throughout the year. Largest differences existed early in spring due to an earlier snow melt in the forest. In the growing season, mean soil temperatures differed by 1.4°C between tundra and forest. The length of the growing season with daily temperatures >3.2°C in the study year was 132 days in tundra and 155 days in the forest. At the treeline, the mean soil temperature was 7.7°C during the growing season. Soil moisture showed no systematic pattern along the elevation transect (*p*_{Elevation} = .34) and no differences between tree canopy and open areas (*p*_{Vegetation} = .94) at the time of sampling in July 2017 (Table S3). Highest values were observed in the middle of the transect 60 m below treeline with gravimetric soil water contents (0–20 cm depth) of 52 ± 5% of moist soils.

3.2 | Plant biomass and litter

Total aboveground tree biomass (foliage, branches, stem, and coarse roots) increased from 2.7 t dry mass ha⁻¹ at the treeline to 36 t dry mass ha⁻¹ in the low elevation forest (95 m below the treeline). Tree biomass N and P stocks followed the same increasing pattern with decreasing elevation (Figure 3). Above treeline, the largest N and P stocks were found in fine roots. Below treeline, N and P stocks increased with decreasing elevation. In low elevation forests, foliage showed the highest N and P stocks among plant biomass pools. Belowground biomass P stocks of coarse and fine roots were rather similar along the gradient, ranging from 0.6 to 0.8 g P m⁻². Understory P stocks ranged from 0.1 to 0.35 g P m⁻² (Figure 3; Table S8). Trends

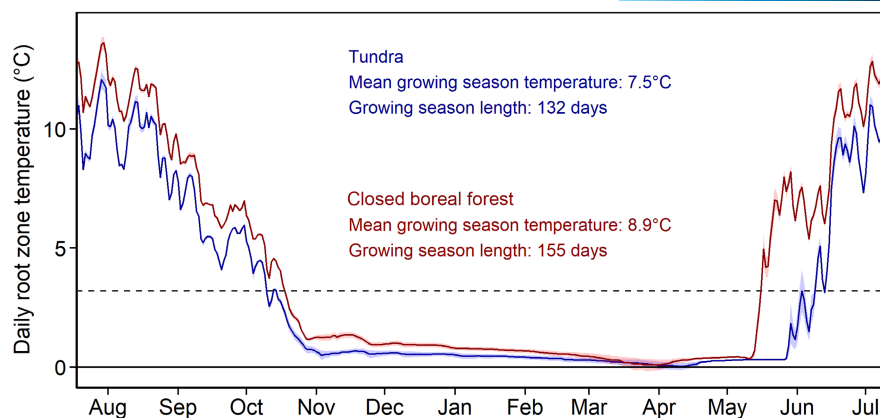


FIGURE 2 Annual course (July 2017 to July 2018) of mean daily soil temperature (rooting zone) measured in high elevation tundra and boreal forest plots at an elevational gradient in the Khibiny Massif, Kola Peninsula, Russia. Mean growing season temperature and growing season length of the vegetation types are shown in red and blue. Shaded areas represent standard error of the mean (tundra: $n=4$, forest: $n=10$). The dashed line indicates the threshold temperature for growing season determination (according to Körner & Paulsen, 2004).

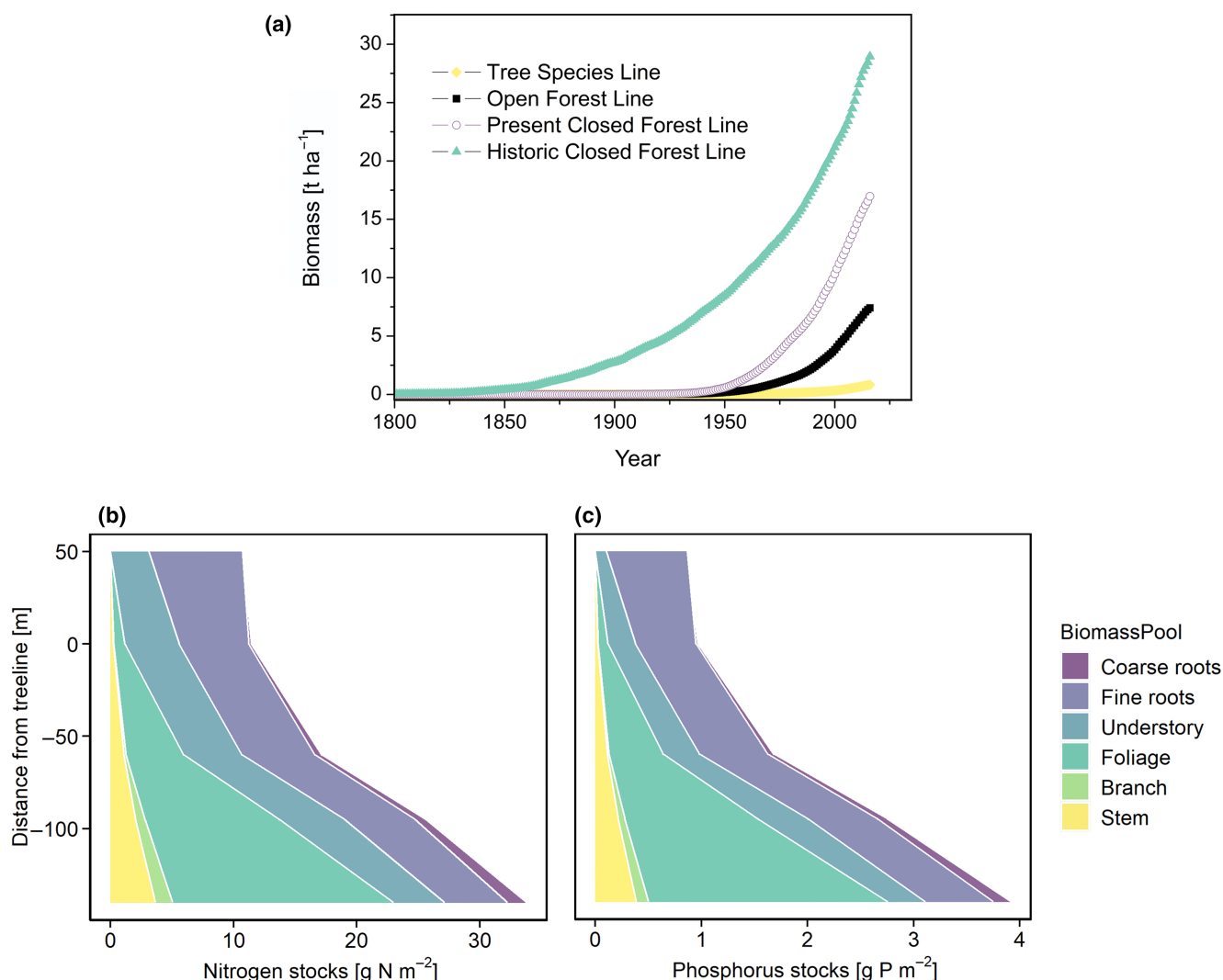


FIGURE 3 (a) Reconstructed changes in aboveground tree biomass since 1800 along the elevational gradient in the Khibiny Massif, Kola Peninsula, Russia, based on dendrochronological data linked to measured tree allometries (Data from Moiseev et al., 2022). (b) Nitrogen and (c) phosphorus stocks in different above- and belowground plant biomass compartments along the same gradients. Further details can be found in Table S8.

were similar for belowground biomass N stocks, with values about an order of magnitude higher compared to P stocks (Figure 3; Table S8).

Foliage N and P concentrations of *B. pubescens* increased with decreasing elevation from treeline to the forest at low elevation from 25 to 40 gN kg⁻¹ and from 2.6 to 4.8 gP kg⁻¹, respectively ($p_{\text{Elevation}} < .06$ and $.01$, Table S5). The foliar mass ratios averaged 17 for C:N, 166 for C:P, and 10 for N:P at treeline. The ratios decreased toward the low elevation forest by a factor of 0.6 ($p_{\text{Elevation}} = .02$, $< .01$, $< .01$, Figure 4). Birch foliage $\delta^{15}\text{N}$ decreased from 1.9‰ in the uppermost trees at the treeline to -4.1‰ at the lowest elevation ($p_{\text{Elevation}} < .01$), but no consistent pattern was found in shed birch litter (Figure 4h). In understory plants, foliar N and P concentrations of *Vaccinium* (*V. myrtillus* and *V. uliginosum*) increased significantly with decreasing elevation ($p_{\text{Elevation}} < .01$).

The dry mass of the litter layer (L and F horizon) increased slightly from $1.7 \pm 0.3 \text{ kg m}^{-2}$ in tundra to $2.0 \pm 0.5 \text{ kg m}^{-2}$ in the forest at low elevation. Litter N and P concentrations increased with decreasing elevation from tundra to forest ($p_{\text{Elevation}} = .04$), with concentrations of P increasing from 0.9 g kg⁻¹ in tundra to 2.7 g kg⁻¹ at the lowest elevation

in the closed forest. Concentrations of N approximately doubled from the highest to the lowest elevation. Accordingly, C:P and C:N ratios in the litter layer decreased toward lower elevations ($p_{\text{Elevation}} < .01$, Figure 4; Table S5). Litter C:N and C:P ratios were consistently lower under tree canopies than in open areas ($p_{\text{Vegetation}} < .01$ and $.03$), with strongest differences at the treeline, where vegetation of open areas was composed of tundra plants. The difference between tree canopy and open areas converged toward lower elevations, especially the litter C:N ratio ($p_{\text{Elevation} \times \text{Vegetation}} < .01$, Figure 4).

3.3 | Mineral soil

Along the elevation gradient, soil depth measured with a soil auger showed a significant increase of 5 cm with decreasing elevation (Figure S2; Table S2). In soil pits, soil depth did not show an elevational pattern (Table S2), averaging $26.4 \pm 8 \text{ cm}$. Soil texture at 10–20 cm depth consisted of 83% sand, 9% silt, and 8% clay. Elevation did not affect soil texture (Table S3). Soil pH decreased

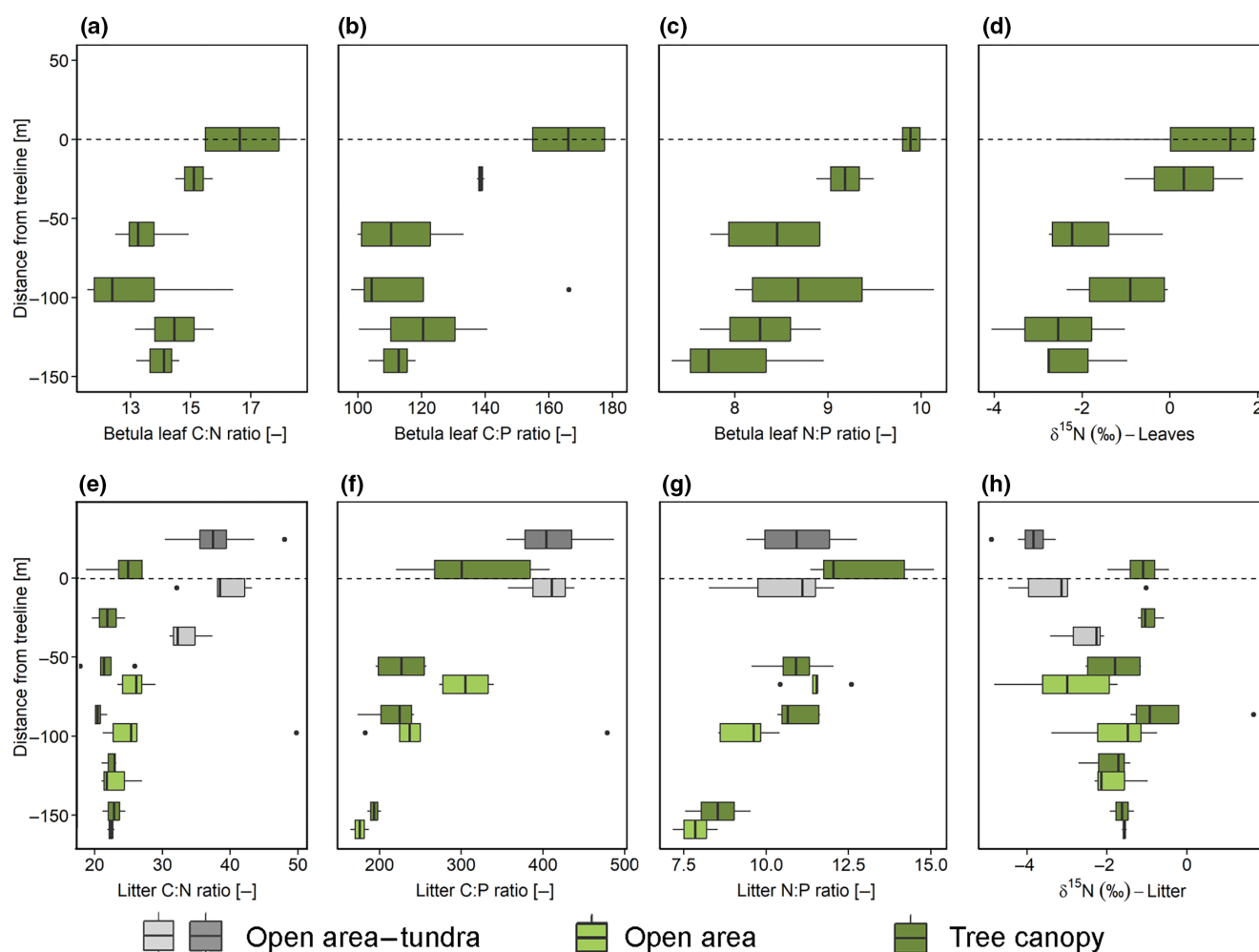


FIGURE 4 Mass ratios of carbon (C), nitrogen (N), and phosphorus (P) concentrations and $\delta^{15}\text{N}$ values of *Betula pubescens* leaves [upper panel, (a–d)] and litter [lower panel (e–h)] sampled in tundra and forest along an elevational gradient in the Khibiny Massif, Kola Peninsula, Russia.

from 4.0 in the tundra to 3.5 in the forest ($p_{\text{Elevation}} = .08$). With soil depth, pH increased ($p_{\text{SoilDepth}} < .01$) from 3.8 at 0–5 cm soil depth to 4.5 at 10–20 cm soil depth. Among plots in open areas in forest patches and below tree canopies, there was no statistically significant difference in soil depth, total nutrient stocks, and stone content.

3.4 | Total C, N, and P contents

3.4.1 | Stones

Major minerals in selected stone samples from all elevational levels were Na-plagioclase (28 weight-%), K-feldspar (24 weight-%), and quartz (22 weight-%). F-apatite contents ranged between 0 and 3 weight-%. Mineral concentrations were similar along the transects. The stone content of soil profiles decreased significantly toward lower elevations ($p_{\text{Elevation}} < .01$, Table S7) from $53 \pm 17 \text{ kg m}^{-2}$ in tundra to $22 \pm 3 \text{ kg m}^{-2}$ in the forest at the lowest elevations. Accordingly, P stocks in stones decreased from tundra ($117 \pm 36 \text{ g P m}^{-2}$) to forest ($49 \pm 7 \text{ g P m}^{-2}$) (Figure 7).

3.4.2 | Fine earth

In contrast to the litter layer, total C, N, and P concentrations in fine earth did not follow a linear trend along the elevational gradient in any soil depth ($p_{\text{Elevation} \times \text{SoilDepth}} < .01$). There was also no statistically significant difference in total C, N, and P concentrations for each elevational level between open area and below tree canopies in any of the soil horizons ($p_{\text{Vegetation}} = .84, .18, .29$, Table S6), but C, N, and P concentrations decreased strongly and continuously with soil depth ($p_{\text{SoilDepth}} < .01$, Table S6). Soil C:N ratios in top- and subsoil increased with decreasing elevation from tundra to the closed forest at low elevation. Soil C:P ratios did not follow a linear trend along the transect, but rather increased from tundra toward former treelines (60–95 m below treeline) and then decreased again toward the low elevation forest in all soil depths, with a decrease toward deeper horizons.

Total fine earth C and N stocks (from litter down to bedrock) showed the smallest stocks in tundra, and increased slightly with decreasing elevation to the closed forests; the increase was, however, not statistically significant ($p_{\text{Elevation}} = .14$ and $.15$, Table 1). Average C and N stocks measured in fine earth were $8.8 \pm 4 \text{ kg C m}^{-2}$ and $0.4 \pm 0.2 \text{ kg N m}^{-2}$, respectively. Separating the topsoil (0–10 cm soil) from subsoil (10 cm soil depth until bedrock) showed a divergent elevation pattern for C and N stocks in top- and subsoils. While in the topsoil C and N stocks declined with decreasing elevation from tundra to forest, they increased in the subsoil (Figures 5 and 6). Total fine earth P stocks increased with decreasing elevation from 0.06 kg m^{-2} in tundra to 0.10 kg m^{-2} in forest, but this increase was not significant ($p_{\text{Elevation}} = .2$). Total fine earth P in the topsoil was highest at the treeline (Figure 6), while subsoil fine earth P stocks consistently increased toward lower elevations.

3.5 | Available N and P contents

Concentrations of KCl-extractable $\text{NH}_4^+\text{-N}$, P_{Resin} , and P_{Bray} increased with decreasing elevation from tundra to the closed forest at all soil depths, with the strongest increase at 0–5 cm soil depth (Figures 6 and 7; Table S6; $p_{\text{Elevation}} < .01$). In the forest, both $\text{NH}_4^+\text{-N}$ and P_{Resin} showed higher concentrations in soils sampled under tree canopies than in open areas ($p_{\text{Vegetation}} < .01$ and $.03$; Table S6). The NO_3^- concentrations in soil extracts remained below detection limits of 0.035 mg L^{-1} .

In contrast to total N and P stocks in the pedon (i.e., fine earth and stones), available nutrient stocks (P_{Resin} , P_{Bray} , and KCl-extractable NH_4) increased strongly with decreasing elevation (Table 1; $p_{\text{Elevation}} < .01$). At 0–10 cm soil depth, stocks of $\text{NH}_4\text{-N}$ and P_{Resin} increased by a factor of 22 and 8 from tundra to the closed forest at low elevation, respectively (Figures 5 and 6). Soils showed on average 3.8 times higher $\text{NH}_4\text{-N}$ stocks under tree canopies than in open areas ($p_{\text{Vegetation}} < .01$; Table 1). At the treeline, soils under the canopies of the uppermost trees had 1.7- and 0.8-time higher stocks of NH_4 and of P_{Resin} as compared to the adjacent open area of the tundra (Table 1), but this effect was only significant for KCl-extractable NH_4 ($p_{\text{Vegetation}} < .05$).

3.6 | Phosphorus stocks in biomass, soils, and stones

Phosphorus stocks in biomass accounted only for ~0.3% of fine earth P stocks at treeline and 1.4% of fine earth P stocks in the low elevation forest (Figure 7). Fine earth P stocks and P in stones were in the same order of magnitude, however, with opposing trends along the elevational transect: In tundra, P stocks were higher in stones than in fine earth, and decreased toward lower elevations, paralleling the increase in soil P (Figure 7). The ratio of stone P stocks in the whole profile to total P stocks in plant and soil was highest in tundra and decreased strongly from 1.8 to 0.5 in the forest at low elevation (Figure 8). The distribution of soil P within the soil profile changed along the transect, decreasing from a ratio of subsoil to topsoil P stock of 1.6 in tundra to 4.1 in the low elevation forest (Figure 8).

3.7 | Microbial biomass, enzymatic activity, and C–N–P-release

Microbial biomass pools of C, N, and P in the soil at 0–10 cm did not change with elevation (Table S4). In contrast, the ratios of microbial C:N, C:P, and N:P became significantly smaller with decreasing elevation from tundra to forest (Figures 5 and 6; Table S4). Potential activities of extracellular enzymes related to the C cycle (β -glucosidase, N-acetyl-glucosaminidase, and xylosidase) upscaled to activity per m^{-2} and soil depth (0–10 cm) was highest in tundra, declining significantly with decreasing elevation ($p_{\text{Elevation}} < .02$; Table S4). Phosphatase activity was also highest in tundra and decreased toward lower elevation forests (Figures 5 and 6; $p_{\text{Elevation}} < .01$). Similarly, potential

TABLE 1 Stocks (mean \pm standard error) of fine earth total carbon (C), nitrogen (N), and phosphorus (P), KCl-extractable ammonium N ($\text{NH}_4^+\text{-N}$) and resin-extractable P (P_{Resin}) along an elevational gradient in the Khibiny Massif, Kola Peninsula, Russia.

Dist. from treeline (m)	Ecosystem	Vegetation	Fine earth C		Fine earth N		Fine earth P ^a		$\text{NH}_4^+\text{-N}$		P_{Resin}	
			g C m^{-2}		g N m^{-2}		g P m^{-2}		g N m^{-2}		g m^{-2}	0.1 m^{-1}
50	Tundra	Open area	7189	± 620	321	± 32	66	± 5	0.04	± 0.01	0.11	± 0.04
0	Treeline	Open area	8290	± 1266	357	± 51	78	± 7	0.09	± 0.04	0.13	± 0.03
		Tree canopy	8393	± 1499	388	± 64			0.10	± 0.04	0.30	± 0.09
-25	Open Forest	Open	9420	± 1816	407	± 81	NA	NA	0.04	± 0.01	0.29	± 0.07
		Tree canopy	7457	± 2681	334	± 121	NA	NA	0.21	± 0.05	0.41	± 0.08
-60	Open Forest	Open area	9345	± 1366	374	± 54	58	± 8	0.25	± 0.15	0.51	± 0.04
		Tree canopy	10,774	± 2945	413	± 100			0.75	± 0.22	0.74	± 0.09
-95	Closed Forest	Open area	9606	± 1665	410	± 68	78	± 9	0.08	± 0.02	0.43	± 0.10
		Tree canopy	8537	± 1342	368	± 54			0.35	± 0.09	0.67	± 0.14
-120	Closed Forest	Open area	9759	± 3149	408	± 127	NA	NA	0.04	± 0.02	0.74	± 0.21
		Tree canopy	9057	± 2938	360	± 111	NA	NA	0.29	± 0.13	0.49	± 0.03
-140	Closed Forest-Old	Open area	10,249	± 2214	451	± 97	102	± 0.2	0.67	± 0.17	1.09	± 0.36
		Tree canopy	11,003	± 2342	490	± 102			1.39	± 0.33	0.67	± 0.17
Statistic			F	p	F	p	F	p	F	p	F	p
Elevation			0.71	.14	2.13	.15	1.87	.20	8.78	<.01	16.89	.01
Vegetation			0.70	.58	0.04	.83	0.19	.66	2.84	<.01	4.86	.10
Elevation*Vegetation			0.63	.79	0.06	.81	0.07	.79	1.30	.26	3.00	.26

Note: Results of linear mixed effects models testing the effects of elevation and vegetation type on response variables are presented. Bold values are $p < .05$.

Abbreviation: NA, not analyzed.

^aFine earth P was measured only at five of seven elevational levels and tree and open samples were pooled due to limited sample amount.

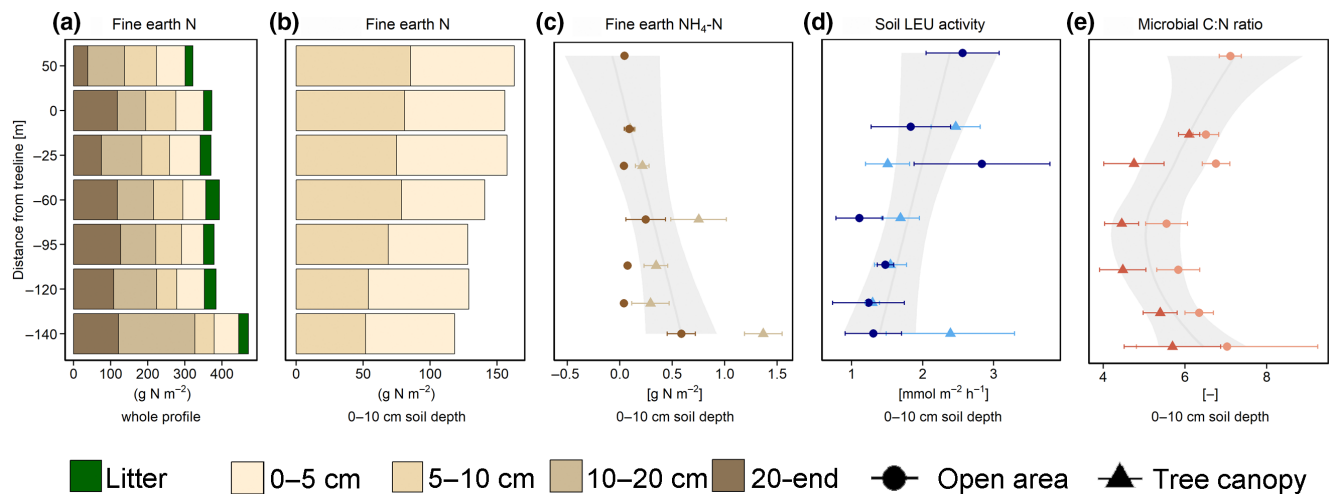


FIGURE 5 Total fine earth nitrogen stocks (a), fine earth nitrogen stocks at 0–10 cm soil depth (b), fine earth KCl-extractable ammonium stocks at 0–10 cm soil depth (c), soil leucine amino-peptidase (LEU) activity at 0–10 cm soil depth (d), and microbial carbon to nitrogen ratios at 0–10 cm soil depth (e) determined along an elevational gradient in the Khibiny Massif, Kola Peninsula, Russia. Sites encompass tundra above treeline, “open areas” and “tree canopy” at treeline and at various elevation in the forest (mean \pm standard error of five plots).

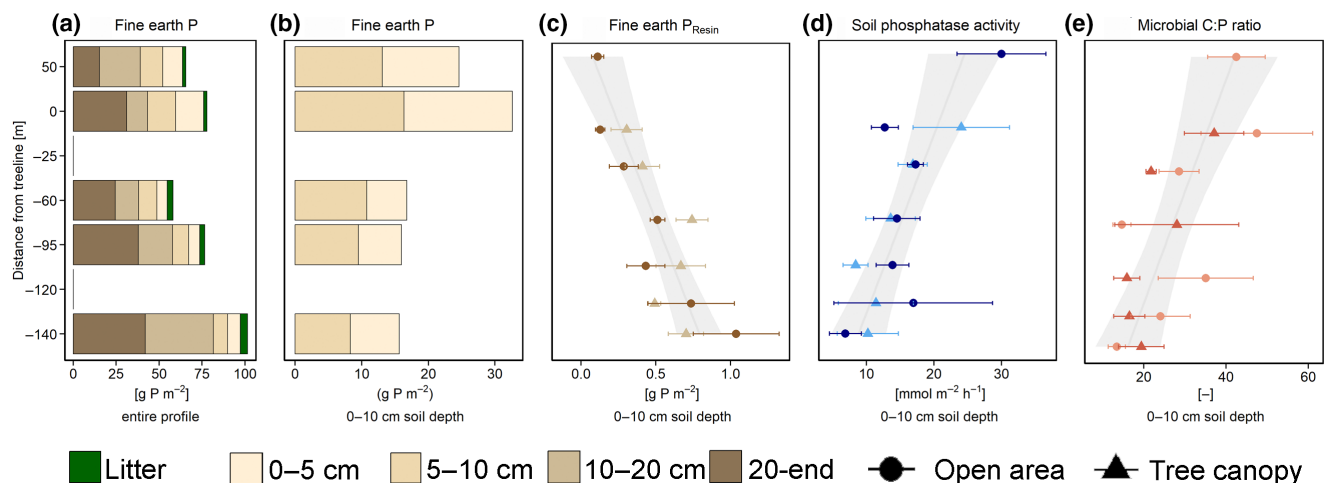


FIGURE 6 Total fine earth phosphorus stocks (a), fine earth phosphorus stocks at 0–10 cm soil depth (b), resin extractable fine earth phosphorus at 0–10 cm soil depth (c), soil phosphatase activity at 0–10 cm soil depth (d), and microbial carbon to phosphorus ratios at 0–10 cm soil depth (e) determined along an elevational gradient in the Khibiny Massif, Kola Peninsula, Russia. Sites encompass tundra above treeline, “open areas” and “tree canopy” at treeline and at various elevation in the forest (mean \pm standard error of five plots).

activity of peptidase declined with declining elevation, but this decline was smaller than for phosphatase and was only marginally significant ($p_{\text{Elevation}} < .1$). As a result, the ratio of peptidase:phosphatase increased significantly from 0.13 in tundra to 0.30 in the low elevation forest ($p_{\text{Elevation}} < .05$, $p_{\text{Elevation} \times \text{Vegetation}} < .05$).

Carbon mineralization from litter and soil during 3 weeks at 15°C showed relatively little differences between tundra and treeline (Figure 9). In contrast, release of NH_4^+ and PO_4^{3-} , reflecting net N and P mineralization, was substantially higher for the litter layer sampled below tree canopies at treeline than under tundra vegetation (NH_4^+ : $p_{\text{Vegetation}} = .02$, PO_4^{3-} : $p_{\text{Vegetation}} = .05$) either 50 m above treeline or adjacent to the trees at treeline (Figure 9). Similar patterns were observed for the incubation of topsoils for net N mineralization, while net P mineralization did not differ between

vegetation types (Figure 9). There was no net NO_3^- release from any sample.

4 | DISCUSSION

4.1 | Improving N and P availability with forest advances

The transects at the Khibiny mountains represent an ideal natural setting to investigate ecosystem C and nutrient pools and cycling in forest–tundra ecotones and to assess how they are affected by climate change-induced vegetation shifts across the treeline. Slopes are even, parent material is similar; soils have identical texture and moisture

contents along the gradient, and soil pH showed a subtle linear decline with decreasing elevation. Moreover, total P stocks in the ecosystem (parent material + fine earth + biomass) remained constant along with elevation. Considering that, during vegetation changes, P is redistributed within the different ecosystem pools and that no P is lost from the ecosystem (e.g., through runoff loss), it is plausible to speculate that inherent site conditions were identical along the entire elevation gradient. We are therefore confident that the observed elevation patterns in N and P cycling are representative for the effects of forest and tundra on nutrient relations. Given that the forest–tundra ecotone has been shifting slowly during the last millennium, lagging behind climate

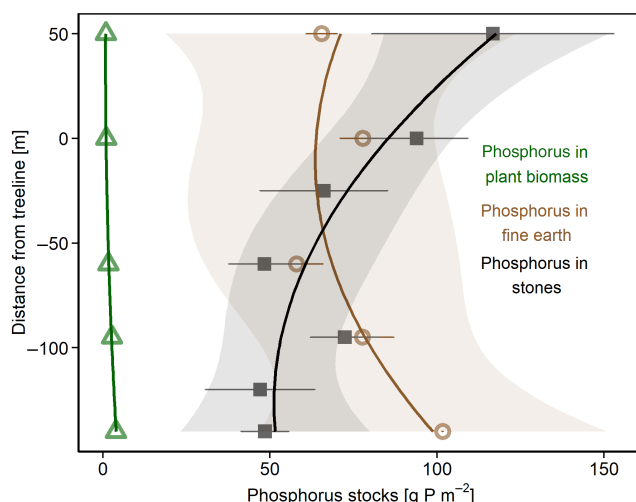


FIGURE 7 Phosphorus stocks (mean \pm standard error) in plant biomass, mineral soil fine earth, and stones along an elevational gradient in the Khibiny Massif, Kola Peninsula, Russia. Stock changes along with elevation are highlighted by applying smoothing splines with shaded areas showing the corresponding 0.95 confidence intervals. Details on plant biomass phosphorus can be found in Figure 3.

changes (Hagedorn et al., 2014; Shiyatov & Mazepa, 2011) and that reconstructed temperature in the Khibiny mountains varied by less than 2.5°C during the last 400 years (Kononov et al., 2009), we are certain that the upper and lower end of the transects had been continuously covered by tundra and forest vegetation for at least centuries. Dendrochronological assessment along the same site revealed that the treeline ecotone has shifted upward by about 70 m in elevation over the last 50–60 years and the open forests became denser (Figure 3; Moiseev et al., 2019, 2022). Consequently, the elevations in between the uppermost and lowest level represent earlier stages of forest expansion into tundra with the uppermost trees being the “leading edge” of forest expanding upward.

Our results reveal that, while total N and P stocks in the ecosystem hardly changed from tundra to the boreal forest at low elevation, the distribution among ecosystem pools was strongly altered. While P pools in parent material decreased from tundra at high elevation to the low elevation forest, N and P pools in biomass and in plant-available form in the soil strongly increased along the same trajectory. This pattern already emerged at the treeline, where soils sampled under the canopies of the uppermost trees showed higher contents of ammonium and plant-available resin P than those sampled in adjacent tundra. This finding at the same elevational level indicates that the positive effects of forest on soil nutrient availability can largely be attributed to the presence of trees and that it goes along with the establishment of trees.

The overall increase in available N and P from tundra toward forest soils is mirrored in increasing nutrient contents in foliage of birch trees and in the two dominant dwarf shrub species of the understory vegetation along the same direction. In agreement, phosphatase and peptidase activity in the soil significantly decreased from tundra to the forest (Figures 5 and 6), suggesting that plants and microbes have to invest less in the production of N and P-acquiring enzymes to meet their nutrient demand. Moreover, the C:N:P ratios in microbial biomass decreased from the tundra toward the forest

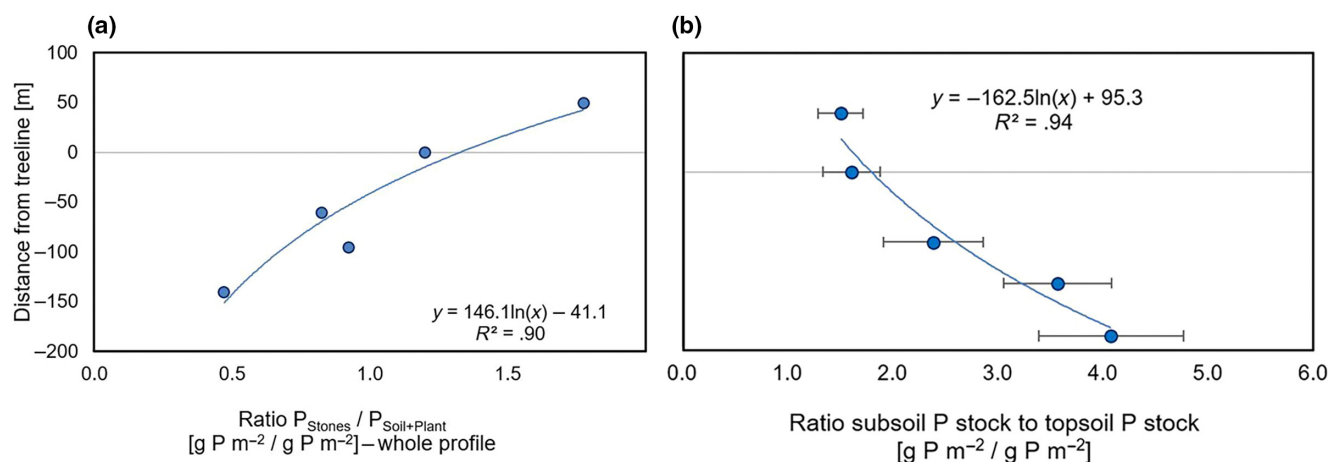


FIGURE 8 Stock ratios of different phosphorus (P) pools along an elevational gradient in the Khibiny Massif, Kola Peninsula, Russia. Ratio of P in stones and P in soil and plant biomass (a); ratio of P in subsoil (>10 cm soil depth, fine earth) and topsoil (litter + 0–10 cm soil depth, fine earth) (b). Ratios of soil P to P_{Resin} and ratios of P in stones to P_{Resin} (Figure S3).

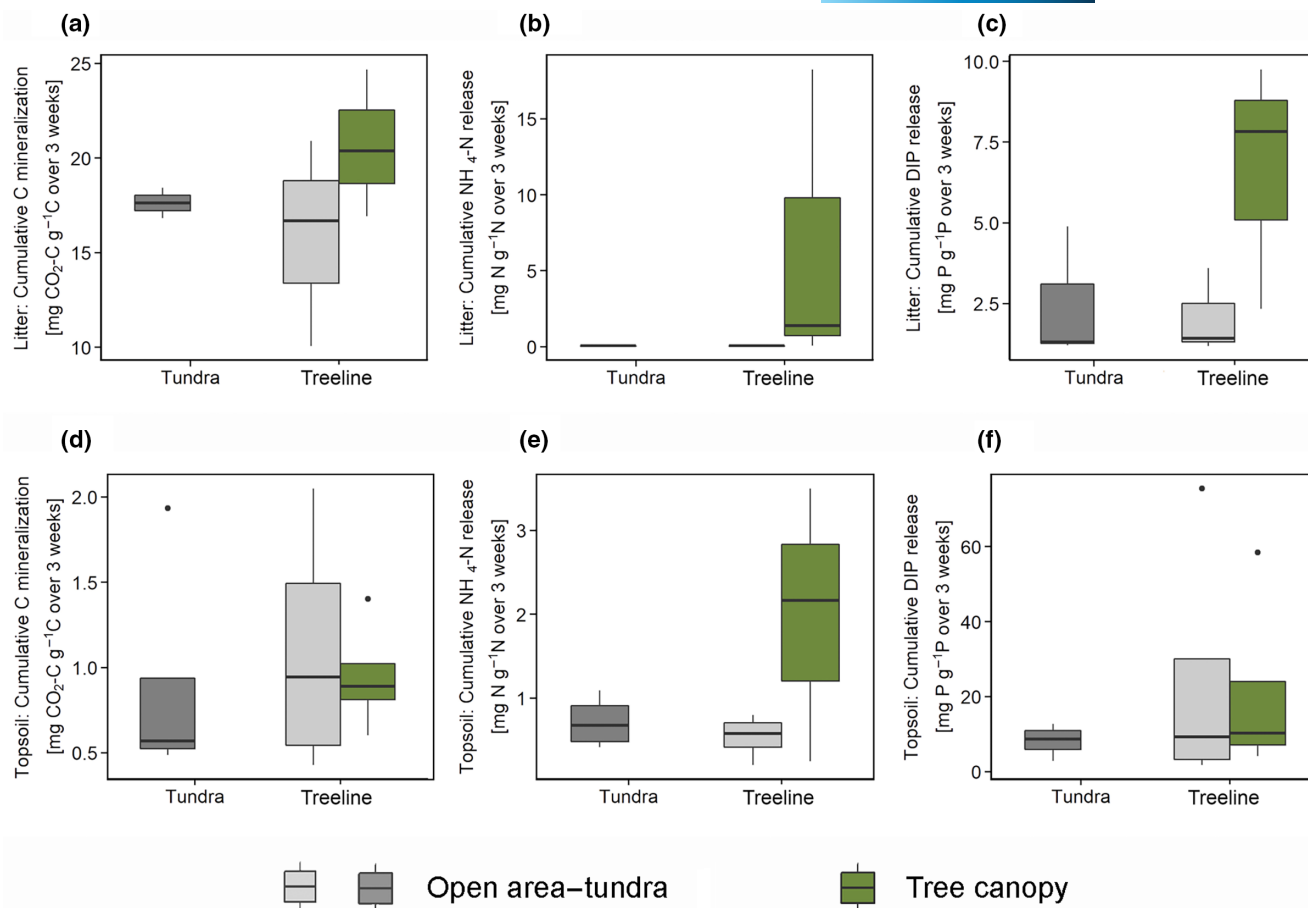


FIGURE 9 Mineralization rate of carbon (C), net release of dissolved ammonium and dissolved inorganic phosphorus (DIP) in litter [upper panel, (a–c)] and 0–5 cm topsoil [lower panel, (d–f)] sampled in tundra and forest along an elevational gradient in the Khibiny Massif, Kola Peninsula, Russia. Forest samples were collected under tree canopies and open areas with tundra plants either in at the highest elevation at tundra or 50 m lower at treeline.

(Figures 5 and 6), which may also be regarded as an adaption of microbial communities to an improving nutrient availability either by adjusting their cellular composition (Camenzind et al., 2021) or by species shifts toward a greater abundance of bacteria as compared to fungi (Strickland & Rousk, 2010).

The increased N availability with forest expansion is in agreement with the observed increases in extractable N contents in the Polar and South Urals (Solly et al., 2017), at Niwot Ridge in the Colorado mountains (Seastedt & Adams, 2001), in Patagonia (Thébault et al., 2014) and in five of seven of the globally studied treelines by Mayor et al. (2017). However, these findings conflict with the results of Clemmensen et al. (2021) in sub-arctic Sweden, where mineral N contents strongly decreased from a heath tundra toward a birch forest. One explanation for the discrepancy could be the contrasting soils with extraordinary shallow mineral soils, but thick organic layers in the Swedish study. Due to the wide C:N ratios and comparatively low N availability in these organic layers, N uptake by trees might have a substantial impact on available N pools in the soils, which in turn requires additional mining for N by ectomycorrhizal fungi, leading to decreasing SOM stocks from heath to birch forests (Clemmensen et al., 2021; Parker et al., 2015). In

comparison, in the Khibiny mountains but also in the Urals (Kammer et al., 2009), mineral soils were comparatively well developed and stored more than 80% of N and total SOM stocks showed even a small increase from tundra to the forest (Table 1).

4.2 | Positive litter feedback

One main reason for the higher soil N and P availability in the low elevation forests than in tundra appears to be the greater N and P release from decomposing organic matter in the forest (Figure 9), which supports our first hypothesis of a positive litter feedback improving nutrient availability with forest expansion. Trees and understory plants in forest produced foliage and litter with significantly narrower C:N:P ratios than in tundra. Consistent with the concept of critical threshold element ratios (Heuck & Spohn, 2016; Mooshammer et al., 2012), the net release of N and P remained negligible in tundra, while it was substantial in the forest. In the mineral soil, C:N and C:P ratios in fine earth did not differ significantly along the elevational gradient and also not between plots below tree canopies and open areas. Soils still showed higher net N release in

the presence of trees. We presume that this apparent conflict arises from the fact that mineralized SOM primarily originates from particulate OM, whose stoichiometry resembles that of litter materials (Hagedorn et al., 2003). Consequently, net N and P release in the soil showed the same pattern as in litter with a strong increase from tundra toward the forest.

What drives plant and litter stoichiometry and consequently, nutrient release from decomposing organic matter? The main reason for the pronounced differences between tundra and forest is very likely a species-specific stoichiometric homeostasis of plant tissues (Elser et al., 2010) with lichens and mosses in the tundra having lower nutrient concentrations than vascular plants (Asplund & Wardle, 2013). Along the transects studied, *B. pubescens* foliage showed rather high nutrient concentrations (on average 33mgN g^{-1} and 3.8mgPg^{-1}), exceeding values for adequate nutrient supply in temperate forests (Hong et al., 2022), which can be attributed to the adaptation of trees against cold conditions (Güsewell, 2004). The narrow N:P ratio of tree foliage (<10) suggests that the nutritional status of trees was better for P than for N, possibly due to the phosphorus-rich parent material, a mafic pluton with high contents of apatite (Kogarko, 2018) and the low soil pH allowing for apatite solubilization. Despite the P-richness of the parent material along the entire gradient, tundra litter remained P poor, released little P upon decomposition, and thus P availability in the soil remained low. Due to the species-specific nature of nutrient dynamics in the plant–soil system (Bowman et al., 2004), we assume that the positive litter feedback as observed here is particularly strong at the studied treeline where a dwarf shrub tundra characterized by low nutrient availability in the soil (Makarov et al., 2019) transitions into a birch forest shedding nutrient-rich broadleaf litter. In contrast, treelines with coniferous trees produce litter with lower nutrient contents (Dawes, Schleppi, Hättenschwiler, et al., 2017), which potentially release little N and P during their decomposition, but further studies are needed to identify the impact of species identity on nutrient dynamics across treelines.

In addition to the positive litter feedback, the more favorable soil climate in the “sheltered” forest than in the “exposed” tundra might have promoted nutrient release and thus, contributed to the increased nutrient availability in the forest (Kammer et al., 2009). In support, a 4°C experimental soil warming at an Alpine treeline induced a 60% increase in KCl-extractable mineral N contents (Dawes, Schleppi, & Hagedorn, 2017). In comparison, measured increases in temperature between tundra and closed forest of the studied treeline were only 1.3°C during the vegetation period and 0.3°C during winter. We therefore assume that direct temperature effects were too small to explain the observed 22- and 8-time increase in available mineral N and P stock in the soil, respectively. Soil moisture could be an additional abiotic driver of nutrient availability which can change across treelines as a result of an altered evapotranspiration and/or the trapping of snow by the forest canopy (Seastedt & Adams, 2001). For the treeline ecotone studied, however, it seems unlikely that soil moisture was important as the Khibiny mountains receive rather high amounts of precipitation (on average 930mm

per year). In agreement, our measurements of gravimetric water contents revealed rather “optimal” water contents of about 50% (per moist soil at 0–20cm depth), and at sampling, soil moisture did not vary significantly with elevation and vegetation across the treeline ecotone. In comparison to net N and P release and against our expectation, C mineralization in the litter layer and soil was only slightly higher ($<30\%$) in the forest than in tundra. Possibly, the positive effects of narrower C:N:P ratios on decomposition were partly outbalanced by greater contents of structural components such as lignin in forest than in tundra litter, which suppresses decomposition (unpublished data; for a general comparison between lichens, mosses, and vascular plants, see Asplund & Wardle, 2013; Hagemann & Moroni, 2015). Although C mineralization in the forest possibly increases with warmer temperatures along the 200m gradient in elevation from tundra toward forest (Figure 2), this increase appears too small to cause the manifold increase in nutrient release and available nutrients in the soil. This further supports the importance of organic matter stoichiometry for the increased release of mineral nutrients toward the forest.

4.3 | Positive weathering feedback

One additional reason for the improving nutrient supply with forest development in the case of P could be enhanced P release and acquisition from bedrock in the forest (Hedin et al., 2003; Prietzel et al., 2013; Richardson et al., 2004). In accordance with our second hypothesis of an increased soil development and weathering from tundra toward forest, soils were about 5cm deeper and less stony in the forest at lower elevation than in tundra. The increase in fine earth is accompanied by a transition in soil type from Leptosols in tundra—a soil type from early development stages, although the area became deglaciated only about 8000years ago—to Podzols in the boreal forest at lower elevation. The advanced weathering in the boreal forest might partly be ascribed to the more favorable soil climate (Hartmann et al., 2014; White et al., 1999) with higher soil temperatures in summer and winter and a 20-day longer growing season in the forest than in tundra (Figure 2). Freeze–thaw cycles might have additionally contributed to weathering (Augusto et al., 2017), although in the year of measurement, soil temperature never dropped below zero along the entire transect (Figure 2). However, it seems likely that trees have additionally promoted weathering as well as nutrient acquisition by their deeper rooting system and their association with ectomycorrhizal fungi. Ectomycorrhizal fungi are regarded as rock-weathering fungi, potentially enhancing the dissolution of P-containing minerals, primarily by the release of low-molecular weight organic acids (Landeweert et al., 2001; Van Breemen, Finlay, et al., 2000; Van Breemen, Lundström, & Jongmans, 2000; Wallander & Hagerberg, 2004). In our study, an increasing activity of ectomycorrhizal fungi with forest densification is supported by decreasing $\delta^{15}\text{N}$ values in tree foliage from treeline toward the boreal forest, which can be attributed to the isotopic fractionation during N transfer from mycorrhizal fungi to host plants

(Hobbie & Högborg, 2012). An additional reason for the enhanced weathering could be a stronger SOM mineralization, promoting the release of protons and soil acidification, which in turn increases the release of P from solubilized apatite and hence, P availability.

Independent on the relative importance of microclimate, rhizosphere mining, or acidification on weathering and soil development, our results strongly suggest that the advanced soil development affected the distribution of P pools. Phosphorus stocks in stones as compared to those in plants and soil fine earth—reflecting P release upon weathering—were almost 50% smaller in forest than in tundra (Figure 8a). The advanced soil development in the low elevation forest is supported by the comparison between sub- and topsoil P (Figure 8b): In the tundra, the ratio is smallest and triples toward the forest at lower elevation. The increase of subsoil P is likely related to the weathering of the parent material, while the decrease of P in the topsoil is likely due to the uptake by plants or to a stronger vertical translocation in the podzolized soil of the boreal forest. The latter is supported by the changing depth distribution of SOM along the elevational gradient. Tundra topsoils (down to 10cm depth) had significantly greater SOC contents than those in the low elevation forest, while subsoils exhibited the opposite trend.

4.4 | Nutrient accumulation in biomass

In support of our third hypothesis, our study documents a strong increase in the binding of N and P in living tree biomass from tundra toward the low elevation forest. Nevertheless, pool sizes of available N and P showed a strong increase with the presence of trees, indicating that positive effects on nutrient availability—by an enhanced nutrient release during organic matter decomposition and from weathering—were quantitatively more important than binding of N and P in tree biomass. Forest biomass P stocks equaled approximately the amount of P extracted by resin in the uppermost 10cm of soil. However, these nutrient amounts accumulated in increasing tree biomass during 120years (when forests started to establish 70m below treeline; Moiseev et al., 2022). Therefore, P binding rates in forest biomass were small as compared to the available P pool in the soil, despite the striking increase of tree biomass P from tundra toward forest. In comparison to P, binding of N in biomass was quantitatively more important. The N storage in forest biomass exceeded the KCl-extractable NH_4 pool in the soil by a factor of 20. Although extractable N represents only a snapshot in time, the pool distribution strongly suggests that binding of N can reduce the available N pool in the soils, thereby tightening N cycling. Ultimately, this may induce a shortage in N, as it has been observed with afforestation and during forest succession in temperate regions, where N accumulation rates in biomass are about a magnitude greater than at treelines (Compton et al., 2007; Lovett et al., 2018; Uri et al., 2007; Vitousek & Reiners, 1975). The comparison of N and P pools in soils and plants strongly suggests that nutrient accumulation in biomass is quantitatively more important for N than for P, which is supported by the decrease of N:P ratios in foliage of birch trees from 9.7 ± 0.2

(mass ratio) at the treeline to 8.1 ± 0.3 in the boreal forest. This suggests that nutrient cycling improves slower with proceeding forest development for N than for P.

4.5 | Summary and implications

Taken together, our results document that treelines represent a natural boundary for N and P cycling in ecosystems with N and P availabilities in the soil showing strong increases from tundra, through the uppermost tree islands emerging at the treeline, to the birch-dominated boreal forest. We presume that the slight temperature changes across the treeline only make a minor direct contribution to the enhanced N and P cycling. Instead, the increased soil N and P availability possibly results from the combined effects of a positive litter feedback with the establishment of trees, a more efficient exploitation of soils by trees, and an enhanced weathering releasing P from stones. These effects apparently outbalance an increased accumulation of nutrients in above- and belowground biomass—hypothesized to “tighten” nutrient cycling with forest succession (Odum, 1969). One reason might be that even in the lowest forest stand 140m below the treeline, tree growth is still slow, and the forest canopy is not closed yet, and therefore, nutrient accumulation in biomass remains relatively low. We can therefore not exclude that the observed improved nutrient availability toward the forest represents only a transient stage; and N and P availabilities ultimately decline with a further accumulation of nutrients in biomass, as observed in forest successions or afforestation on former grass- and cropland under more favorable climatic conditions with faster growing trees (Compton et al., 2007; Lovett et al., 2018; Weber & Bardgett, 2011). The consideration of boreal forests as nutrient-poor ecosystems (Augusto et al., 2017) would support this notion.

The increase in soil N and P availability from tundra toward forest observed here and at other treelines (Mayor et al., 2017) and the improved nutritional status of microbes and plants strongly suggest a shift from an organic to an inorganic nutrient economy (DeForest & Snell, 2020) from tundra toward forest. This potentially impacts treeline dynamics in a warming climate. Once trees are established, the positive effect on soil fertility might have contributed to the densification of forests during the last decades (Moiseev et al., 2019) and the strong growth enhancement below treeline with a 5- to 10-fold increase in forest stand productivity within a 100-m decline in elevation (Hagedorn et al., 2020). Conversely, the very low nutrient availability in tundra may impede the establishment of trees at the “leading edge,” thereby contributing to the retarded treeline advances in a changing climate.

AUTHOR CONTRIBUTIONS

Jasmin Fetzer: Formal analysis; investigation; project administration; visualization; writing – original draft; writing – review and editing. **Pavel Moiseev:** Conceptualization; investigation; methodology; writing – review and editing. **Emmanuel Frossard:** Supervision; writing – review and editing. **Klaus Kaiser:** Resources; supervision; writing – review

and editing. **Mathias Mayer:** Writing – review and editing. **Konstantin Gavazov:** Formal analysis; investigation; writing – review and editing. **Frank Hagedorn:** Conceptualization; funding acquisition; investigation; methodology; supervision; writing – review and editing.

ACKNOWLEDGMENTS

We gratefully acknowledge the financial support by the Swiss National Science Foundation (SNF) for JF and FH (project number 171171) and for KG (project number PZ00P2_174047), as well as by the German Research Foundation (DFG) for JF and KK under the Priority Program SPP 1685 “Ecosystem nutrition: Forest strategies for limited phosphorus resources” (grant KA1673/9-2). MM was supported by an Erwin Schrödinger Fellowship from the Austrian Science Fund FWF (project no. J-4369) and by a personal research grant from the ETH Board awarded to Andreas Rigling. We thank the WSL central laboratory (A. Schlumpf, K. v. Känel, J. Bollenbach, U. Graf, D. Pezzotta), the WSL forest soil laboratory (A. Zürcher, B. Rahimi, D. Christen, N. Hajjar), and our interns M. Zapata, K. McKeve, M. Roca, and Yo-Ho Tseng for chemical analyses and support. Special thanks to P. Winkler at the Halle soil laboratory and Michael Plötze from ETH Zürich for XRF and XRD analyses. This work was performed within the framework of the joint projects conceived by the Institute of Plant and Animal Ecology of the Ural Branch of the Russian Academy of Science (IPAE) and the Swiss Federal Institute for Forest, Snow, and Landscape Research (WSL). Open access funding provided by ETH-Bereich Forschungsanstalten.

CONFLICT OF INTEREST STATEMENT

The authors declare no conflict of interest.

DATA AVAILABILITY STATEMENT

The data that support the findings of this study are openly available in EnviDat at <https://doi.org/10.16904/envidat.476>.

ORCID

Jasmin Fetzer  <https://orcid.org/0000-0002-6889-7745>

Pavel Moiseev  <https://orcid.org/0000-0003-4808-295X>

Emmanuel Frossard  <https://orcid.org/0000-0002-8345-2330>

Klaus Kaiser  <https://orcid.org/0000-0001-7376-443X>

Mathias Mayer  <https://orcid.org/0000-0003-4366-9188>

Konstantin Gavazov  <https://orcid.org/0000-0003-4479-7202>

Frank Hagedorn  <https://orcid.org/0000-0001-5218-7776>

REFERENCES

- Asplund, J., & Wardle, D. A. (2013). The impact of secondary compounds and functional characteristics on lichen palatability and decomposition. *Journal of Ecology*, 101(3), 689–700. <https://doi.org/10.1111/1365-2745.12075>
- Augusto, L., Achat, D. L., Jonard, M., Vidal, D., & Ringeval, B. (2017). Soil parent material—A major driver of plant nutrient limitations in terrestrial ecosystems. *Global Change Biology*, 23(9), 3808–3824. <https://doi.org/10.1111/gcb.13691>
- Bates, D., Mächler, M., Bolker, B., & Walker, S. (2015). Fitting linear mixed-effects models using lme4. *Journal of Statistical Software*, 67(1), 1–48. <https://doi.org/10.18637/jss.v067.i01>
- Bowman, W. D., Steltzer, H., Rosenstiel, T. N., Cleveland, C. C., & Meier, C. L. (2004). Litter effects of two co-occurring alpine species on plant growth, microbial activity and immobilization of nitrogen. *Oikos*, 104(2), 336–344. <https://doi.org/10.1111/j.0030-1299.2004.12721.x>
- Brödl, D., Kaiser, K., & Hagedorn, F. (2019). Divergent patterns of carbon, nitrogen, and phosphorus mobilization in forest soils. *Frontiers in Forests and Global Change*, 2, 66. <https://doi.org/10.3389/ffgc.2019.00066>
- Brödl, D., Kaiser, K., Kessler, A., & Hagedorn, F. (2019). Drying and rewetting foster phosphorus depletion of forest soils. *Soil Biology and Biochemistry*, 128, 22–34. <https://doi.org/10.1016/j.soilbio.2018.10.001>
- Camenzind, T., Philipp Grenz, K., Lehmann, J., & Rillig, M. C. (2021). Soil fungal mycelia have unexpectedly flexible stoichiometric C:N and C:P ratios. *Ecology Letters*, 24(2), 208–218. <https://doi.org/10.1111/ele.13632>
- Celi, L., Cerli, C., Turner, B. L., Santoni, S., & Bonifacio, E. (2013). Biogeochemical cycling of soil phosphorus during natural revegetation of *Pinus sylvestris* on disused sand quarries in northwestern Russia. *Plant and Soil*, 367(1–2), 121–134. <https://doi.org/10.1007/s11104-013-1627-y>
- Clemmensen, K. E., Durling, M. B., Michelsen, A., Hallin, S., Finlay, R. D., & Lindahl, B. D. (2021). A tipping point in carbon storage when forest expands into tundra is related to mycorrhizal recycling of nitrogen. *Ecology Letters*, 24, 1193–1204. <https://doi.org/10.1111/ele.13735>
- Compton, J. E., Hooker, T. D., & Perakis, S. S. (2007). Ecosystem N distribution and $\delta^{15}\text{N}$ during a century of forest regrowth after agricultural abandonment. *Ecosystems*, 10(7), 1197–1208. <https://doi.org/10.1007/s10021-007-9087-y>
- Dawes, M. A., Philipson, C. D., Fonti, P., Bebi, P., Hättenschwiler, S., Hagedorn, F., & Rixen, C. (2015). Soil warming and CO_2 enrichment induce biomass shifts in alpine tree line vegetation. *Global Change Biology*, 21(5), 2005–2021. <https://doi.org/10.1111/gcb.12819>
- Dawes, M. A., Schleppi, P., & Hagedorn, F. (2017). The fate of nitrogen inputs in a warmer alpine treeline ecosystem: A ^{15}N labelling study. *Journal of Ecology*, 105(6), 1723–1737. <https://doi.org/10.1111/1365-2745.12780>
- Dawes, M. A., Schleppi, P., Hättenschwiler, S., Rixen, C., & Hagedorn, F. (2017). Soil warming opens the nitrogen cycle at the alpine treeline. *Global Change Biology*, 23(1), 421–434. <https://doi.org/10.1111/gcb.13365>
- DeForest, J. L., & Snell, R. S. (2020). Tree growth response to shifting soil nutrient economy depends on mycorrhizal associations. *New Phytologist*, 225(6), 2557–2566. <https://doi.org/10.1111/nph.16299>
- Elser, J. J., Fagan, W. F., Kerkhoff, A. J., Swenson, N. G., & Enquist, B. J. (2010). Biological stoichiometry of plant production: Metabolism, scaling and ecological response to global change. *New Phytologist*, 186(3), 593–608. <https://doi.org/10.1111/j.1469-8137.2010.03214.x>
- Fox, J., Weisberg, S., Price, B., Adler, D., Bates, D., Baud-Bovy, G., & Bolker, B. (2019). *car: Companion to applied regression*.
- Gee, G. W., & Bauder, J. W. (1986). Particle-size analysis. In A. Klute (Ed.), *Methods of soil analysis* (2nd ed., pp. 1149–1178). American Society of Agronomy, Inc., Soil Science Society of America, Inc.
- German, D. P., Weintraub, M. N., Grandy, A. S., Lauber, C. L., Rinkes, Z. L., & Allison, S. D. (2011). Optimization of hydrolytic and oxidative enzyme methods for ecosystem studies. *Soil Biology and Biochemistry*, 43(7), 1387–1397. <https://doi.org/10.1016/j.soilbio.2011.03.017>
- Güsewell, S. (2004). N:P ratios in terrestrial plants: Variation and functional significance. *New Phytologist*, 164(2), 243–266. <https://doi.org/10.1111/j.1469-8137.2004.01192.x>
- Hagedorn, F., Dawes, M. A., Bubnov, M. O., Devi, N. M., Grigoriev, A. A., Mazepa, V. S., Nagimov, Z. Y., Shiyatov, S. G., & Moiseev, P. A. (2020). Latitudinal decline in stand biomass and productivity at the

- elevational treeline in the Ural mountains despite a common thermal growth limit. *Journal of Biogeography*, 47(8), 1827–1842. <https://doi.org/10.1111/jbi.13867>
- Hagedorn, F., Gavazov, K., & Alexander, J. M. (2019). Above- and below-ground linkages shape responses of mountain vegetation to climate change. *Science*, 365(6458), 1119–1123. <https://doi.org/10.1126/science.aax4737>
- Hagedorn, F., Shiyatov, S. G., Mazepa, V. S., Devi, N. M., Grigo'ev, A. A., Bartysh, A. A., Fomin, V. V., Kapralov, D. S., Terent'ev, M., Bugman, H., Rigling, A., & Moiseev, P. A. (2014). Treeline advances along the Urals mountain range – Driven by improved winter conditions? *Global Change Biology*, 20(11), 3530–3543. <https://doi.org/10.1111/gcb.12613>
- Hagedorn, F., Spinnler, D., Bundt, M., Blaser, P., & Siegwolf, R. (2003). The input and fate of new C in two forest soils under elevated CO₂. *Global Change Biology*, 9(6), 862–872. <https://doi.org/10.1046/j.1365-2486.2003.00638.x>
- Hagemann, U., & Moroni, M. T. (2015). Moss and lichen decomposition in old-growth and harvested high-boreal forests estimated using the litterbag and minicontainer methods. *Soil Biology and Biochemistry*, 87, 10–24. <https://doi.org/10.1016/j.soilbio.2015.04.002>
- Harsch, M. A., Hulme, P. E., McGlone, M. S., & Duncan, R. P. (2009). Are treelines advancing? A global meta-analysis of treeline response to climate warming. *Ecology Letters*, 12(10), 1040–1049. <https://doi.org/10.1111/j.1461-0248.2009.01355.x>
- Hartmann, J., Moosdorf, N., Lauerwald, R., Hinderer, M., & West, A. J. (2014). Global chemical weathering and associated P-release – The role of lithology, temperature and soil properties. *Chemical Geology*, 363, 145–163. <https://doi.org/10.1016/j.chemgeo.2013.10.025>
- Hedin, L. O., Vitousek, P. M., & Matson, P. A. (2003). Nutrient losses over four million years of tropical forest development. *Ecological Research*, 84(9), 2231–2255. <https://doi.org/10.1890/02-4066>
- Hedley, M. J., & Stewart, J. W. B. (1982). Method to measure microbial in soils. *Soil Biology & Biochemistry*, 14, 377–385.
- Heuck, C., & Spohn, M. (2016). Carbon, nitrogen and phosphorus net mineralization in organic horizons of temperate forests: Stoichiometry and relations to organic matter quality. *Biogeochemistry*, 131, 229–242. <https://doi.org/10.1007/s10533-016-0276-7>
- Hobbie, E. A., & Höglberg, P. (2012). Nitrogen isotopes link mycorrhizal fungi and plants to nitrogen dynamics. *New Phytologist*, 196(2), 367–382. <https://doi.org/10.1111/j.1469-8137.2012.04300.x>
- Hong, D. S., Gonzales, K. E., Fahey, T. J., & Yanai, R. D. (2022). Foliar nutrient concentrations of six northern hardwood species responded to nitrogen and phosphorus fertilization but did not predict tree growth. *PeerJ*, 10, e13193. <https://doi.org/10.7717/peerj.13193>
- Kammer, A., Hagedorn, F., Shevchenko, I., Leifeld, J., Guggenberger, G., Goryacheva, T., Rigling, A., & Moiseev, P. (2009). Treeline shifts in the Ural mountains affect soil organic matter dynamics. *Global Change Biology*, 15(6), 1570–1583. <https://doi.org/10.1111/j.1365-2486.2009.01856.x>
- Kogarko, L. (2018). Chemical composition and petrogenetic implications of apatite in the Khibiny Apatite-Nepheline deposits (Kola Peninsula). *Minerals*, 8(11), 532. <https://doi.org/10.3390/min8110532>
- Kononov, Y. M., Friedrich, M., & Boettger, T. (2009). Regional summer temperature reconstruction in the Khibiny Low Mountains (Kola Peninsula, NW Russia) by means of tree-ring width during the last four centuries. *Arctic, Antarctic, and Alpine Research*, 41(4), 460–468. <https://doi.org/10.1657/1938-4246-41.4.460>
- Körner, C., & Paulsen, J. (2004). A world-wide study of high altitude treeline temperatures. *Journal of Biogeography*, 31(5), 713–732. <https://doi.org/10.1111/j.1365-2699.2003.01043.x>
- Kuznetsova, A., Brockhoff, P. B., & Christensen, R. H. B. (2017). lmerTest package: Tests in linear mixed effects models. *Journal of Statistical Software*, 82(13), 1–26. <https://doi.org/10.18637/jss.v082.i13>
- Landeweert, R., Hoffland, E., Finlay, R. D., Kuyper, T. W., & Van Breemen, N. (2001). Linking plants to rocks: Ectomycorrhizal fungi mobilize nutrients from minerals. *Trends in Ecology & Evolution*, 16(5), 248–254. [https://doi.org/10.1016/S0169-5347\(01\)00212-X](https://doi.org/10.1016/S0169-5347(01)00212-X)
- Liang, E., Wang, Y., Piao, S., Lu, X., Camarero, J. J., Zhu, H., Zhu, L., Ellison, A. M., Ciais, P., & Peñuelas, J. (2016). Species interactions slow warming-induced upward shifts of treelines on the Tibetan Plateau. *Proceedings of the National Academy of Sciences of the United States of America*, 113(16), 4380–4385. <https://doi.org/10.1073/pnas.1520582113>
- Lovett, G. M., Goodale, C. L., Ollinger, S. V., Fuss, C. B., Ouimet, A. P., & Likens, G. E. (2018). Nutrient retention during ecosystem succession: A revised conceptual model. *Frontiers in Ecology and the Environment*, 16(9), 532–538. <https://doi.org/10.1002/fee.1949>
- Makarov, M. I., Buzin, I. S., Tiunov, A. V., Malysheva, T. I., Kadulin, M. S., & Koroleva, N. E. (2019). Nitrogen isotopes in soils and plants of tundra ecosystems in the Khibiny Mountains. *Eurasian Soil Science*, 52(10), 1195–1206. <https://doi.org/10.1134/S1064229319100077>
- Mathisen, I. E., Mikheeva, A., Tutubalina, O. V., Aune, S., & Hofgaard, A. (2014). Fifty years of tree line change in the Khibiny Mountains, Russia: Advantages of combined remote sensing and dendroecological approaches. *Applied Vegetation Science*, 17(1), 6–16. <https://doi.org/10.1111/avsc.12038>
- Mayor, J. R., Sanders, N. J., Classen, A. T., Bardgett, R. D., Clément, J. C., Fajardo, A., Lavorel, S., Sundqvist, M. K., Bahn, M., Chisholm, C., Cieraad, E., Gedalof, Z., Grigulis, K., Kudo, G., Oberski, D. L., & Wardle, D. A. (2017). Elevation alters ecosystem properties across temperate treelines globally. *Nature*, 542(7639), 91–95. <https://doi.org/10.1038/nature21027>
- Möhl, P., Mörsdorf, M. A., Dawes, M. A., Hagedorn, F., Bebi, P., Viglietti, D., Freppaz, M., Wipf, S., Körner, C., Thomas, F. M., & Rixen, C. (2018). Twelve years of low nutrient input stimulates growth of trees and dwarf shrubs in the treeline ecotone. *Journal of Ecology*, 107, 768–780. <https://doi.org/10.1111/1365-2745.13073>
- Moir, J., & Tiessen, H. (2007). Characterization of available P by sequential extraction. In M. R. Carter (Ed.), *Soil sampling and methods of analysis* (2nd ed., pp. 75–86). CRC Press. <https://doi.org/10.1201/9781420005271.ch25>
- Moiseev, P. A., Galimova, A. A., Bubnov, M. O., Devi, N. M., & Fomin, V. V. (2019). Tree stands and their productivity dynamics at the upper growing limit in Khibiny on the background of modern climate changes. *Russian Journal of Ecology*, 50(5), 431–444. <https://doi.org/10.1134/S1067413619050084>
- Moiseev, P. A., Hagedorn, F., Balakin, D. S., Bubnov, M. O., Devi, N. M., Kukarskih, V. V., Mazepa, V. S., Viyukhin, S. O., Viyukhina, A. A., & Grigoriev, A. A. (2022). Stand biomass at treeline ecotone in Russian subarctic mountains is primarily related to species composition but its dynamics driven by improvement of climatic conditions. *Forests*, 13(2), 254. <https://doi.org/10.3390/f13020254>
- Mooshammer, M., Wanek, W., Schneckner, J., Wild, B., Hofhansl, F., Blöchl, A., Hämmerle, I., Frank, A. H., Fuchslueger, L., Keiblinger, K. M., Zechmeister-Boltenstern, S., & Richter, A. (2012). Stoichiometric controls of nitrogen and phosphorus cycling in decomposing beech leaf litter. *Ecology*, 93(4), 770–782.
- Mooshammer, M., Wanek, W., Zechmeister-Boltenstern, S., & Richter, A. (2014). Stoichiometric imbalances between terrestrial decomposer communities and their resources: Mechanisms and implications of microbial adaptations to their resources. *Frontiers in Microbiology*, 5, 1–10. <https://doi.org/10.3389/fmicb.2014.00022>
- Odum, E. P. (1969). The strategy of ecosystem development. *Science*, 164, 203–216. https://doi.org/10.5822/978-1-61091-491-8_20
- Ohno, T., & Zibilske, L. M. (1991). Determination of low concentrations of phosphorus in soil extracts using malachite green. *Soil Science Society of America Journal*, 55, 892–895.

- Parker, T. C., Subke, J. A., & Wookey, P. A. (2015). Rapid carbon turnover beneath shrub and tree vegetation is associated with low soil carbon stocks at a subarctic treeline. *Global Change Biology*, 21(5), 2070–2081. <https://doi.org/10.1111/gcb.12793>
- Pekala, K. (1998). Nival moraines and rock glaciers in the Khibiny mts (the Kola Peninsula). *Geomorfologia*, 137–145.
- Pepin, N., Bradley, R. S., Diaz, H. F., Baraer, M., Caceres, E. B., Forsythe, N., Fowler, H., Greenwood, G., Hashmi, M. Z., Liu, X. D., Miller, J. R., Ning, L., Ohmura, A., Palazzi, E., Rangwala, I., Schoner, W., Severskiy, I., Shahgedanova, M., Wang, M. B., ... Yang, D. Q. (2015). Elevation-dependent warming in mountain regions of the world. *Nature Climate Change*, 5(5), 424–430. <https://doi.org/10.1038/nclimate2563>
- Prietz, J., Dümig, A., Wu, Y., Zhou, J., & Klysubun, W. (2013). Synchrotron-based P K-edge XANES spectroscopy reveals rapid changes of phosphorus speciation in the topsoil of two glacier foreland chronosequences. *Geochimica et Cosmochimica Acta*, 108, 154–171. <https://doi.org/10.1016/j.gca.2013.01.029>
- Pritsch, K., Courty, P. E., Churin, J. L., Cloutier-Hurteau, B., Ali, M. A., Damon, C., Duchemin, M., Egli, S., Ernst, J., Fraissinet-Tachet, L., Kuhar, F., Legname, E., Marmesse, R., Müller, A., Nikolova, P., Peter, M., Plassard, C., Richard, F., Schloter, M., ... Garbaye, J. (2011). Optimized assay and storage conditions for enzyme activity profiling of ectomycorrhizae. *Mycorrhiza*, 21(7), 589–600. <https://doi.org/10.1007/s00572-011-0364-4>
- R Core Team. (2020). *R: A language and environment for statistical computing*. R Foundation for Statistical Computing. <https://www.r-project.org/>
- Richardson, S. J., Peltzer, D. A., Allen, R. B., McGlone, M. S., & Parfitt, R. L. (2004). Rapid development of phosphorus limitation in temperate rainforest along the Franz Josef soil chronosequence. *Oecologia*, 139(2), 267–276. <https://doi.org/10.1007/s00442-004-1501-y>
- Seastedt, T. R., & Adams, G. A. (2001). Effects of mobile tree islands on alpine tundra soils. *Ecology*, 82(1), 8–17.
- Shiyatov, S. G., & Mazepa, V. S. (2011). Climate-driven dynamics of the forest-tundra vegetation in the Polar Ural Mountains. *Contemporary Problems of Ecology*, 4(7), 758–768. <https://doi.org/10.1134/S1995425511070071>
- Solly, E. F., Djukic, I., Moiseev, P. A., Andreyashkina, N. I., Devi, N. M., Göransson, H., Mazepa, V. S., Shiyatov, S. G., Trubina, M. R., Schweingruber, F. H., Wilmking, M., & Hagedorn, F. (2017). Treeline advances and associated shifts in the ground vegetation alter fine root dynamics and mycelia production in the South and Polar Urals. *Oecologia*, 183(2), 571–586. <https://doi.org/10.1007/s00442-016-3785-0>
- Strickland, M. S., & Rousk, J. (2010). Considering fungal:bacterial dominance in soils – Methods, controls, and ecosystem implications. *Soil Biology and Biochemistry*, 42(9), 1385–1395. <https://doi.org/10.1016/j.soilbio.2010.05.007>
- Sullivan, P. F., Ellison, S. B. Z., McNown, R. W., Brownlee, A. H., & Sveinbjörnsson, B. (2015). Evidence of soil nutrient availability as the proximate constraint on growth of treeline trees in northwest Alaska. *Ecology*, 96(3), 716–727. <https://doi.org/10.1890/14-0626.1>
- Thébault, A., Clément, J. C., Ibanez, S., Roy, J., Geremia, R. A., Pérez, C. A., Buttler, A., Estienne, Y., & Lavelle, S. (2014). Nitrogen limitation and microbial diversity at the treeline. *Oikos*, 123(6), 729–740. <https://doi.org/10.1111/j.1600-0706.2013.00860.x>
- Uri, V., Vares, A., Tullus, H., & Kanai, A. (2007). Above-ground biomass production and nutrient accumulation in young stands of silver birch on abandoned agricultural land. *Biomass and Bioenergy*, 31(4), 195–204. <https://doi.org/10.1016/j.biombioe.2006.08.003>
- Ushakova, G. I., Shmakova, N. Y., & Koroleva, N. E. (2003). Spatial analysis of soils, vegetation, productivity, and carbon stored in mountain tundra ecosystems, Khibiny Mountains, Russia. *Polar Geography*, 27(3), 210–224. <https://doi.org/10.1080/789610168>
- Van Breemen, N., Finlay, R., Lundström, U., Jongmans, A. G., Giesler, R., & Olsson, M. (2000). Mycorrhizal weathering: A true case of mineral plant nutrition? *Biogeochemistry*, 49(1), 53–67. <https://doi.org/10.1023/A:1006256231670>
- Van Breemen, N., & Finzi, A. C. (1998). Plant–soil interactions: Ecological aspects and evolutionary implications. *Biogeochemistry*, 42, 1–19. <https://doi.org/10.1023/A:1005996009413>
- Van Breemen, N., Lundström, U. S., & Jongmans, A. G. (2000). Do plants drive podzolization via rock-eating mycorrhizal fungi? *Geoderma*, 94(2–4), 163–171. [https://doi.org/10.1016/S0016-7061\(99\)00050-6](https://doi.org/10.1016/S0016-7061(99)00050-6)
- Vitousek, P. M., & Reiners, W. A. (1975). Ecosystem succession and nutrient retention: A hypothesis. *Bioscience*, 25(6), 376–381. <https://doi.org/10.2307/1297148>
- Wallander, H., & Hagerberg, D. (2004). Do ectomycorrhizal fungi have a significant role in weathering of minerals in forest soil? *Symbiosis*, 37(1–3), 249–257.
- Wang, L., Chen, Y., Zhou, Y., Zheng, H., Xu, Z., Tan, B., You, C., Zhang, L., Li, H., Guo, L., Wang, L., Huang, Y., & Liu, Y. (2021). Litter chemical traits strongly drove the carbon fractions loss during decomposition across an alpine treeline ecotone. *Science of the Total Environment*, 753, 142287. <https://doi.org/10.1016/j.scitotenv.2020.142287>
- Weber, P., & Bardgett, R. D. (2011). Influence of single trees on spatial and temporal patterns of belowground properties in native pine forest. *Soil Biology & Biochemistry*, 43, 1372–1378. <https://doi.org/10.1016/j.soilbio.2011.03.015>
- Welc, M., Frossard, E., Egli, S., Bünemann, E. K., & Jansa, J. (2014). Rhizosphere fungal assemblages and soil enzymatic activities in a 110-years alpine chronosequence. *Soil Biology and Biochemistry*, 74, 21–30. <https://doi.org/10.1016/j.soilbio.2014.02.014>
- White, A. F., Blum, A. E., Bullen, T. D., Vivit, D. V., Schulz, M., & Fitzpatrick, J. (1999). The effect of temperature on experimental and natural chemical weathering rates of granitoid rocks. *Geochimica et Cosmochimica Acta*, 63(19–20), 3277–3291. [https://doi.org/10.1016/S0016-7037\(99\)00250-1](https://doi.org/10.1016/S0016-7037(99)00250-1)
- WRB. (2014). *World reference base for soil resources*. <https://www.fao.org/3/i3794en/i3794en.pdf>

SUPPORTING INFORMATION

Additional supporting information can be found online in the Supporting Information section at the end of this article.

How to cite this article: Fetzer, J., Moiseev, P., Frossard, E., Kaiser, K., Mayer, M., Gavazov, K., & Hagedorn, F. (2024). Plant–soil interactions alter nitrogen and phosphorus dynamics in an advancing subarctic treeline. *Global Change Biology*, 30, e17200. <https://doi.org/10.1111/gcb.17200>

Supplementary material

Soil profiles along the transect

Distance
from
treeline [m]

Soil

Understory

Tundra 50



Tree
line 0



Boreal
Forest -25



Boreal
Forest -60



Boreal
Forest -95



Boreal
Forest -120



Boreal
Forest -140



Figure S1: Representative photographs of the soil profiles and understory vegetation for each elevational level.

Table S1: Characterization of the vegetation within the elevational transect

Tundra:	
Dwarf shrubs:	<i>Vaccinium uliginosum</i> , <i>Vaccinium myrtillus</i> , <i>Betula nana</i> <i>Empetrum hermaphroditum</i> , <i>Dryas octopetala</i> , <i>Arctostaphylos alpine</i> , <i>Arctostaphylos uva-ursi</i> , <i>Salix polaris</i> , <i>S. herbacea</i> , <i>Loiseleuria procumbens</i> , <i>Harrimanella hypnoides</i>
Grasses:	<i>Carex bigelowii</i> , <i>Festuca ovina</i> , <i>Cassiope tetragona</i> , <i>Ledum palustre</i> , <i>Diapensia lapponica</i> , <i>Luzula arcuate</i> , <i>Silene acaulis</i>
Mosses:	<i>Polytrichum piliferum</i> , <i>Racomitrium lanuginosum</i> , <i>Dicranum spp.</i> , <i>Pleurozium schreberi</i> , <i>Ptilidium ciliare</i>
Lichens:	<i>Cetraria islandica</i> , <i>Cladonia stellaris</i> , <i>Flavocetraria nivalis</i> , <i>Nephroma arcticum</i> , <i>Alectoria ochroleuca</i>
Treeline dominant species:	
	<i>Betula pubescens ssp. czerepanovii</i>
Low elevation forest:	
	<i>Betula pubescens ssp. Czerepanovii</i> and <i>Picea obovata Ledeb</i>

Danilova A.D., Koroleva N.E., Novakovsky A.B. Differentiation of flora and vegetation of the tundra and fjell field in Khibiny and Lovozero massif (Kola Peninsula). Transactions of the Kola Science Centre of RAS. Series: Natural Sciences and Humanities. 2022. Vol. 1, No. 2. P. 129–139.

Soil depth along the transect

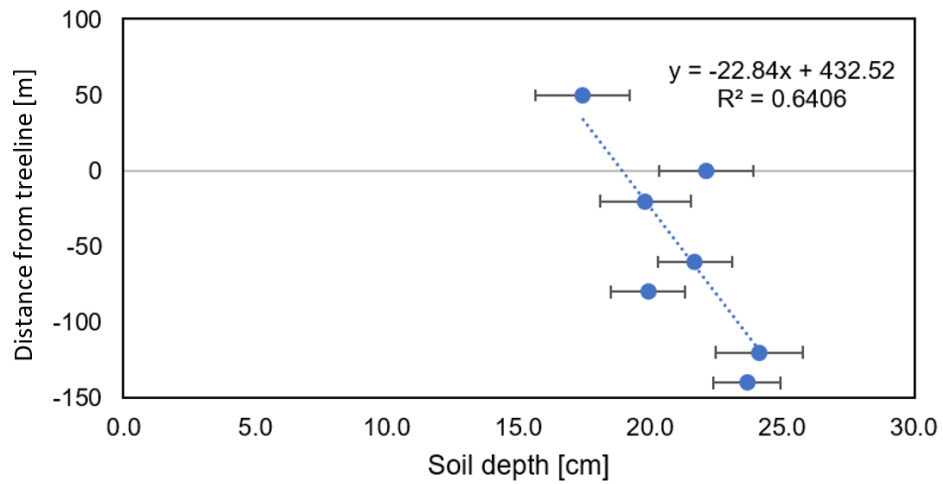


Figure S2: Mean soil depth with standard error for each elevation level measured with a soil auger.

Table S2: Mean soil depth with standard error for each elevation level, measured (A) with a soil auger and (B) in the soil pits.

A

Distance from treeline [m]	50	0	-25	-60	-95	-120	-140
Average [cm]	17.43	22.10	19.81	21.68	19.91	24.14	23.68
STDEV	14.85	14.62	14.06	12.09	11.69	12.75	10.25
SE	1.79	1.79	1.72	1.41	1.41	1.67	1.27
n	69	67	67	73	69	58	65

B

Distance from treeline [m]	50	0	-25	-60	-95	-120	-140
Average [cm]	28.03	28.89	23.20	24.72	32.02	23.46	24.72
STDEV	7.86	8.21	8.17	6.22	9.56	9.45	8.09
SE	1.29	1.22	1.63	0.93	1.37	1.75	1.18
n	37	45	25	45	49	29	47

Table S3: Soil texture, pH-values, and P_{Bray} in the soil of 0-10 cm depth and gravimetric water content (GWC) in the soil of 0-20 cm depth sampled under tree canopies or open areas along the gradient from tundra at high elevation to the boreal forest at low elevation. Means and standard errors are given. Statistical significances of the fixed effects Elevation, Vegetation (Open area vs. Tree canopy), and their interaction were estimated with linear mixed-effect model.

Elevation from treeline	Eco-system	Vegetation	Sand %	Silt %	Clay %	pH		GWC (0-20 cm, in %)		P_{Bray} (0-10 cm) mg P/(m ² *0.1m)	
						Mean	SE	Mean	SE		
50	Tundra	Open	86	6	8	3.98	±0.11	43.9	3.8	138	±43
0	Treeline	Open	84	8	9	4.03	±0.15	45.5	2.3	147	±72
		Tree	88	6	6	4.10	±0.11	42.7	2.9	274	±120
-25	New	Open	86	6	8	3.80	±0.14	41.1	6.8	325	±172
	Forest	Tree	87	8	5	3.65	±0.11	36.4	0.3	310	±23
-60	New	Open	79	10	11	3.51	±0.10	49.2	5.3	467	±57
	Forest	Tree	77	10	13	3.75	±0.16	52.4	6.5	630	±75
-95	Older	Open	81	10	9	3.87	±0.19	40.2	5.3	407	±192
	Forest	Tree	83	11	6	3.89	±0.06	39.2	2.3	480	±81
-120	Older	Open	85	7	9	3.47	±0.17	43.9	0.2	684	±262
	Forest	Tree	83	10	7	3.71	±0.11	42.9	3.7	380	±22
-140	Old	Open	77	16	7	3.59	±0.09	36.1	2.1	896	±473
	Forest	Tree	81	13	6	3.99	±0.09	37.0	0.3	700	±171
Statistics						F	p	F	p	F	p
Elevation			n.d.	n.d.	n.d.	3.41	0.09	0.99	0.34	26.2	0.002
Vegetation			n.d.	n.d.	n.d.	0.01	0.94	0.01	0.94	1.3	0.35
Elevation x Vegetation			n.d.	n.d.	n.d.	0.27	0.61	0.1	0.76	0.74	0.47

bold indicate p -values < 0.05

Table S4: Microbial biomass carbon, nitrogen, and phosphorus (stocks), ratios of microbial C:N:P, potential activity of carbon related enzymes as the sum of β -glucosidase, N-acetyl-glucosaminidase, and xylosidase, and the ratio of peptidase-to-phosphatase in the soil of 0-10 cm depth sampled under tree canopies or open areas along the gradient from tundra at high elevation to the boreal forest at low elevation. Means and standard errors are given. Statistical significances of the fixed effects Elevation, Vegetation (Tree vs. Open), and their interaction were estimated with linear mixed-effect model.

Elevation from treeline	Eco-system	Vegetation	MB-C gC/(m ² *0.1m)		MB-N gN/(m ² *0.1m)		MB-P P/(m ² *0.1m)		Microbial C:N		Microbial C:P		Microbial N:P		C-related enzyme activity mmol/(m ² *h)		Peptidase-to-phosphatase activity	
50	Tundra	Open	2751	±403	407	±68	119	±27	6.94	±0.31	27.9	±3.8	4.07	±0.56	166.8	±29.9	0.10	±0.02
0	Treeline	Open	3666	±687	626	±143	141	±38	6.17	±0.53	29.2	±5.8	5.18	±1.57	112.2	±13.4	0.14	±0.03
		Tree	2388	±449	413	±86	90	±13	5.90	±0.31	26.6	±4.6	4.48	±0.63	164.2	±42.3	0.13	±0.03
-25	New	Open	2468	±496	359	±48	108	±14	6.79	±0.54	23.2	±4.4	3.36	±0.39	154.0	±24.1	0.15	±0.05
	Forest	Tree	2085	±9.7	462	±103	99	±9	4.87	±1.07	21.4	±2.1	4.89	±1.49	125.4	±30.3	0.09	±0.01
-60	New	Open	2614	±394	495	±57	217	±35	5.26	±0.47	12.7	±2.1	2.39	±0.30	120.3	±22.4	0.09	±0.02
	Forest	Tree	3100	±792	761	±197	215	±44	4.19	±0.47	14.4	±2.5	3.42	±0.37	106.3	±23.4	0.19	±0.07
-95	Older	Open	2123	±812	365	±111	174	±46	5.56	±0.66	11.4	±2.6	2.02	±0.36	72.4	±21.0	0.12	±0.02
	Forest	Tree	1741	±314	483	±99	175	±41	3.92	±0.64	12.6	±3.8	3.13	±0.49	77.6	±15.6	0.20	±0.03
-120	Older	Open	2215	±301	371	±75	121	±30	6.13	±0.61	20.2	±4.0	3.40	±0.80	124.4	±42.9	0.07	±0.01
	Forest	Tree	2750	±1006	582	±258	163	±79	5.10	±0.43	18.8	±2.3	4.18	±0.25	90.7	±30.3	0.17	±0.05
-140	Old	Open	961	±197	255	±119	86	±25	6.13	±2.55	12.1	±1.7	2.80	±0.77	66.9	±33.6	0.17	±0.05
	Forest	Tree	2234	±971	485	±204	118	±32	5.87	±2.45	20.5	±6.7	3.96	±1.04	46.2	±52.8	0.41	±0.06
Statistics			F	p	F	p	F	p	F	p	F	p	F	p	F	p	F	p
Elevation			4.3	0.047	0.17	0.69	1.14	0.29	8.1	0.008	13.87	0.0008	5.66	0.024	10.6	0.017	6.1	0.048
Vegetation			0.74	0.4	4.8	0.04	0.01	0.94	4.97	0.038	0.57	0.46	6.31	0.021	0.07	0.78	10.4	0.004
Elevation x Vegetation			3.53	0.075	2.15	0.16	1.6	0.22	0	0.94	0.79	0.38	0.49	0.49	0.86	0.36	8.6	0.008

bold indicate p-values<0.05

Table S5: Foliage and litter data and results of linear-mixed effect models (model <- lmer(SoilC.N ~ Elevation * Vegetation + (1|Transect/ ElevLevel), REML = T, data = logS_D1) of element contents of foliage of *Betula pubescens* and of the litter layer sampled under tree canopies or open areas along the gradient from tundra at high elevation to the boreal forest at low elevation.

Elevation from treeline	Eco- system	Vege- tation	Betula Foliage N	Betula Foliage P	Betula Foliage C:N	Betula Foliage C:P	Betula Foliage N:P	Betula Foliage δ15N	Litter layer N	Litter layer P	Litter layer C:N	Litter layer C:P	Litter layer N:P	Litter layer δ15N
			mg N kg ⁻¹	mg P kg ⁻¹	-	-	-	‰	g N kg ⁻¹	g P kg ⁻¹	-	-	-	‰
50	Tundra	Open							11.78	1.07	37.97	412.07	10.96	-3.89
0	Treeline	Open							11.58	1.10	38.82	404.35	10.54	-3.11
		Tree	28272.50	2853.49	16.81	166.33	9.90	0.54	19.60	1.55	24.28	316.17	12.89	-1.15
-25	New	Open							13.96	NA	33.56	NA	NA	-2.58
	Forest	Tree	31515.00	3431.16	15.11	138.60	9.18	0.32	21.22	NA	22.00	NA	NA	-0.95
-60	New	Open							18.37	1.60	25.93	298.48	11.51	-3.02
	Forest	Tree	34972.50	4192.45	13.49	113.51	8.39	-1.84	21.56	1.99	21.72	236.01	10.87	-1.82
-95	Older	Open							16.86	1.81	29.08	274.54	9.41	-1.80
	Forest	Tree	36125.00	4137.08	13.19	118.26	8.87	-1.05	22.84	2.10	20.02	219.58	10.95	-0.43
-120	Older	Open							19.42	NA	23.29	NA	NA	-1.81
	Forest	Tree	32390.00	3966.85	14.46	120.50	8.27	-2.55	20.31	NA	22.12	NA	NA	-1.56
-140	Old	Open							18.75	2.41	22.44	175.78	7.85	-1.56
	Forest	Tree	32996.67	4140.05	13.98	111.46	8.00	-2.17	19.67	2.32	22.87	193.54	8.54	-1.62
			F-value	F-value	F-value	F-value	F-value	F-value	F-value	F-value	F-value	F-value	F-value	F-value
Elevation			4.04†	10.31**	13.2**	0.69	1.14	0.29	7.24*	77.0***	11.0**	54.52***		2.44
Vegetation			n.d.	n.d.	n.d.	n.d.	n.d.	n.d.	55.84***	11.0**	46.54***	5.36*		35.06***
Elevation x Vegetation			n.d.	n.d.	n.d.	n.d.	n.d.	n.d.	18.5**	2.0	14.81**	0.237		12.22**

Significance levels †p<0.10; *p<0.05; **p<0.01; ***p<0.001; bold indicate p-values<0.05

Table S6: Results of linear mixed effect model of soil nutrient concentrations for all soil layers.

	SoilC_log				SoilN_log				SoilP_log			
	DF	F value	p value		DF	F value	p value		DF	F value	p value	
Elevation	1	0.421	0.53		1	0.881	0.37		1	0.973	0.35	
Soil depth	4	88.986	<0.01	**	4	76.017	<0.01	**	4	36.441	<0.01	**
Vegetation	1	0.042	0.84		1	1.835	0.18		1	1.146	0.29	
Elevation x Soil depth	4	8.238	<0.01	**	4	11.617	<0.01	**	4	39.065	<0.01	**
Elevation x Vegetation	1	0.088	0.77		1	1.04	0.31		1	0.29	0.59	
Soil depth: Vegetation	4	0.687	0.60		4	1.86	0.12		4	1.968	0.10	
Elevation x Soil depth x Vegetation	4	0.367	0.83		4	0.71	0.59		4	1.846	0.12	
	NH4.N_log				ResinP_log				Soil15N			
	DF	F value	p value		DF	F value	p value		DF	F value	p value	
Elevation	1	8.112	0.01	*	1	10.407	<0.01	**	1	0.196	0.66	
Soil depth	2	3.011	0.05	+	1	109.439	<0.01	**	4	404.66	<0.01	**
Vegetation	1	12.146	<0.01	**	1	4.803	0.03	*	1	2.836	0.10	
Elevation x Soil depth	2	11.534	<0.01	**	1	0.873	0.35		4	3.645	<0.01	**
Elevation Vegetation	x 1	0.056	0.81		1	1.29	0.26		1	1.526	0.22	
Soil depth: Vegetation	2	7.825	<0.01	**	1	1.859	0.18		4	7.699	<0.01	**
Elevation x Soil depth x Vegetation	2	3.438	0.04	*	1	0.744	0.39		4	2.662	0.03	*
	MBC_log				MBN_log				MBP_log			
	DF	F value	p value		DF	F value	p value		DF	F value	p value	
Elevation	1	2.572	0.13		1	0.605	0.45		1	1.291	0.28	
Soil depth	1	55.934	<0.01	**	1	100.18	<0.01	**	1	52.976	<0.01	***
Vegetation	1	0.134	0.72		1	0.425	0.52		1	0.208	0.65	
Elevation x Soil depth	1	0.138	0.71		1	0.755	0.39		1	0.759	0.39	
Elevation Vegetation	x 1	1.359	0.25		1	0.787	0.38		1	0.053	0.82	
Soil depth: Vegetation	1	0.351	0.56		1	0.008	0.93		1	0.053	0.82	
Elevation x Soil depth x Vegetation	1	1.993	0.16		1	1.31	0.26		1	0.267	0.61	

Significance levels †p<0.10; *p<0.05; **p<0.01; bold indicate p-values<0.05

Table S7: Results of linear mixed effect models of soil properties and carbon and nutrient stocks.

	SoilDepth					SoilMass				logStones			
	DF	F value	p value			DF	F value	p value			DF	F value	p value
Elevation	1	0.14	0.71		1	7.30	0.02	*	1	9.29	<0.01	**	
Vegetation	1	0.15	0.70		1	1.11	0.30		1	0.22	0.64		
Elevation x Vegetation	1	0.23	0.63		1	0.50	0.48		1	0.15	0.70		
	logSoilC					SoilN				logSoilP			Sign.
	DF	F value	p value			DF	F value	p value			DF	F value	
Elevation	1	2.30	0.14		1	2.13	0.15		1	1.87	0.20		
Vegetation	1	0.31	0.58		1	0.04	0.83		1	0.19	0.66		
Elevation x Vegetation	1	0.07	0.79		1	0.06	0.81		1	0.07	0.79		
	log_ResinP					log_NH4.N							
	DF	F value	p value			DF	F value	p value			DF	F value	p value
Elevation	1	16.89	<0.01	***	1	8.78	0.01	**					
Vegetation	1	4.86	0.03	*	1	2.84	0.10	+					
Elevation x Vegetation	1	3.00	0.09	+	1	1.30	0.26						
	log_Ptase					log_LEU							
	DF	F value	p value			DF	F value	p value			DF	F value	p value
Elevation	1	15.33	<0.01	***	1	2.17	0.16						
Vegetation	1	0.07	0.79		1	0.14	0.71						
Elevation x Vegetation	1	0.19	0.67		1	0.90	0.35						

Significance levels †p<0.10; *p<0.05; **p<0.01; ***p<0.001; bold indicate p-values<0.05

Phosphorus and nitrogen stocks in different biomass and soil pools

Table S8: Nitrogen (N) and phosphorus (P) concentrations and stocks in different above- and belowground compartments along the elevational transect

			Tundra	sparse treeline	open forest	current closed forest	past closed forest	Data Source	Reference
Nitrogen			0	1	3	5	7		
Level									
Tree									
Biomass	Total	g/m ²	0	160	760	1530	2750	this site	Moiseev et al. (2022)
	Foliage	g/m ²		31.9	148.7	302.9	544.5	this site	Moiseev et al. (2022)
	Branches	g/m ²		7.0	31.5	127.2	228.6	this site	Moiseev et al. (2022)
	Stem	g/m ²		121.1	579.8	1099.9	1976.9	this site	Moiseev et al. (2022)
	Coarse roots	g/m ²		108.2	291.8	469.7	844.3	Ratio above/below for Betula forest at treeline in Northern Ural	Hagedorn et al. (2020)
	Fine roots	g/m ²	661	491	424.5	400	300	Average South and Polar Ural	Solly et al. (2017)
	Understory- foliage	g/m ²	100	100	100	100	80	Average South and Polar Ural	Solly et al. 2017
	Understory- branches	g/m ²	400	400	400	400	300	Ratio between foliage and branches	Dawes et al. (2015)
N conc.	N-foliage	mgN/g		28.27	31.52	36.13	33.00	This study	Uri (2007)
	N-branches	mgN/g		6.06	6.06	6.06	6.06		
	N-Stem	mgN/g		1.85	1.85	1.85	1.85	This study	
	N-coarse roots	mgN/g		1.85	1.85	1.85	1.85	Assumed to correspond to wood	Solly et al. (2017)
	N-Fine roots	mgN/g	11.50	11.50	13.95	14.33	17.00	Average South and Polar Ural	
	N-Understory Foliage	mgN/g	11.06	24.20	27.41	32.97	33.27	This study	
	N- Understory- branches	mgN/g	5	5	5	5	5	estimated from Dawes et al. (2015)	
N Pools	N-foliage	gN/m ²	0.00	0.90	4.69	10.94	17.97		
	N-branches	gN/m ²	0.00	0.04	0.19	0.77	1.38		
	N-Stem	gN/m ²	0.00	0.22	1.07	2.03	3.65		
	N-Coarse Roots	gN/m ²	0.00	0.20	0.54	0.87	1.56		
	N-Fine Roots	gN/m ²	7.60	5.65	5.92	5.73	5.10		
	N Understory	gN/m ²	3.11	4.42	4.74	5.30	4.16		
	Total N- Biomass	gN/m ²	10.71	11.43	17.15	25.64	33.82		
P conc.	P-Foliage	mgP/kg		2853.5	3431.2	4137.1	4140.1	This study	Uri (2007)
	P-branches	mgP/kg		493.0	493.0	493.0	493.0		
	P-stem	mgP/kg		196.3	196.3	196.3	196.3	This study	
	P-coarse roots	mgP/kg		196.3	196.3	196.3	196.3	based on N concentrations and N:P ratio of foliage	based on N concentrations assuming the N:P ratio of foliage
	P-fine roots	mgP/g	1150.0	1160.7	1518.8	1640.5	2133.0		

N and P dynamics in a treeline ecotone - Supplementary material

	P-Understory Foliage	mgP/kg	1052.4	2588.7	3421.6	4731.4	4433.2	This study based on N concentrations assuming the N:P ratio of foliage
	P-Understory Branches	mgP/kg	500	500	500	500	500	
P Pools	P-Foliage	gP/m ²	0.000	0.091	0.510	1.253	2.254	
	P-branches	gP/m ²	0.000	0.003	0.016	0.063	0.113	
	P-stem	gP/m ²	0.000	0.024	0.114	0.216	0.388	
	P-coarse roots	gP/m ²	0.000	0.021	0.057	0.092	0.166	
	P-fine roots	gP/m ²	0.760	0.570	0.645	0.656	0.640	
	P-understory	gP/m ²	0.105	0.259	0.342	0.473	0.355	
	Total P Biomass	gP/m ²	0.865	0.968	1.684	2.753	3.915	
	Tree-biomass		0.000	0.118	0.640	1.532	2.755	
	Below-ground biomass		0.760	0.591	0.702	0.748	0.806	
	Total N:P ratio		12.37	11.81	10.18	9.31	8.64	

Ratio of different phosphorus pools along the transect

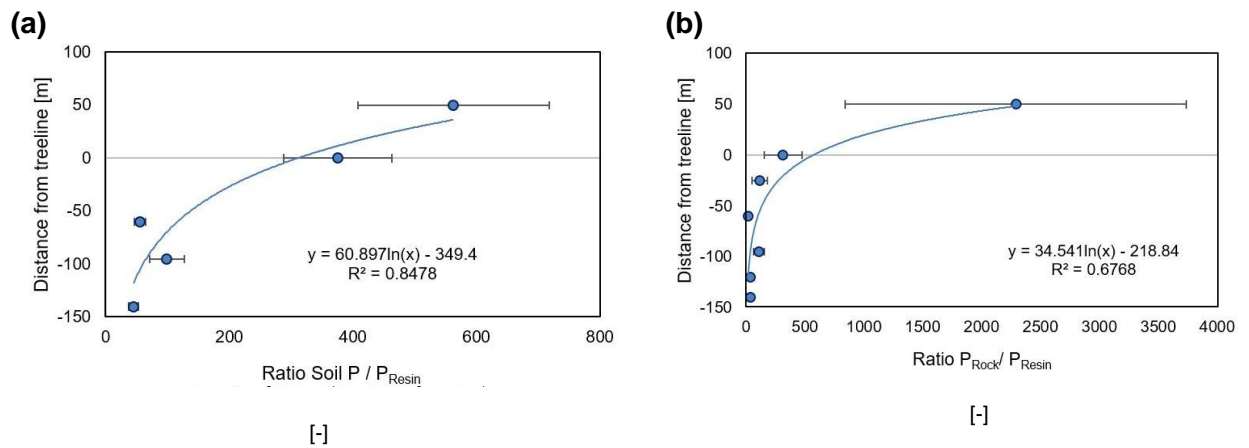


Figure S3: Ratios of phosphorus (P) stocks of different P pools along the elevational transect. (a) Ratio of total soil P to resin extractable soil P (P_{Resin}); (b) Ratio of skeleton P to resin extractable P.